CONCEPTUAL DESIGN AND PHYSICAL MODEL TESTS OF A LEVEE-IN-DUNE HURRICANE BARRIER

A Thesis

by

NICHOLAS ALLAN WEST

Submitted to the Office of Graduate and Professional Studies of
Texas A&M University
in partial fulfillment of the requirements for the degree of
MASTER OF SCIENCE

Chair of Committee,	Scott Socolofsky
Co-Chair of Committee,	Jens Figlus
Committee Members,	James Kaihatu
	Chris Houser
Head of Department,	Robin Autenrieth

December 2014

Major Subject: Ocean Engineering

ABSTRACT

In an effort to protect the Greater Houston Metropolitan Area from hurricane storm surge damage, four Levee-in-Dune concepts are studied as part of the Ike Dike project. The Ike Dike is a proposed hurricane surge barrier developed by Dr. William Merrell at Texas A&M University at Galveston and is based on best practices developed by the Dutch. The project would span 62 mi including a levee system along the Galveston and Bolivar coasts, and a channel barrier across Bolivar Roads. This design study includes a homogeneous sand dune, and three dunes that each incorporate different protective cores: an armorstone revetment core, a clay levee core, and a concrete T-Wall core. The concepts undergo physical model tests that subject them to conditions that simulate 100-year storm damage caused by both surge and waves. Dune and beach morphology for each concept is measured through laser profiling techniques, and each concept is evaluated based on calculated erosion and accretion, as well as design considerations including cost. Wave conditions are measured by capacitance gauges at several locations. The Clay-Core and T-Wall concepts proved to be the most effective barriers against hurricane storm surge and wave protection based on their endurance during testing.

ACKNOWLEDGEMENTS

First and foremost, I would like to thank Prof. Jens Figlus. Thank you for giving me the opportunity to work with you on such an important and interesting project, and for all of your guidance along the way. Thank you for all the time you spent in the lab with me, and all of your enthusiastic support as my mentor.

Next, I would like to extend my fullest gratitude to Dr. William Merrell for the idea of the Ike Dike, and for putting together the resources and people necessary to make this project happen.

I would also like to thank Prof. Scott Socolofsky for all of his help in making my research in Galveston possible and Prof. James Kaihatu and Prof. Chris Houser for sitting on my committee and giving me invaluable insight and feedback.

Thank you Robert Tyler and Jake Sigren for countless hours in the flume shoveling sand, building dunes, collecting data and fixing hardware. Without you, I would never have finished this project.

Thank you to all my family and friends who were there to give me support throughout my entire time at Texas A&M.

The work presented in this thesis was part of the project Barrier Design and Landscape Integration for Galveston's West End funded by the Coastal Beach and Bay Foundation.

NOMENCLATURE

GHMA	Greater Houston Metropolitan Area
LID	Levee-In-Dune
CPF	Coastal Processes Flume
TAMUG	Texas A&M University, Galveston Campus
MSL	Mean Sea Level
NAVD88	North American Vertical Datum of 1988
USACE	United States Army Corps of Engineers
GoM	Gulf of Mexico
GMP	Gross Metropolitan Product
BEA	Bureau of Economic Analysis
USCB	United States Census Bureau
HSDRRS	Hurricane and Storm Damage Risk Reduction System
h_d	Dune Height
w_d	Dune Width
h_l	Levee Height
w_l	Levee Width
t	Sand Layer Thickness
Θ	Dune Slope
s_m	Model Scale Factor
k	Wavenumber
λ_p	Peak Wavelength
H_s	Significant Wave Height
H_m	Mean Wave Height
h	Water Depth
T_p	Peak Wave Period
T_s	Significant Wave Period
D_{50}	Median Diameter
M_{50}	Median Mass
V	Volume
ρ	Density
g	Gravitational Acceleration

ΔDF_x	Dune Face X-Location Change
S_x	Submerged Beach Profile X-Location
S_h	Submerged Beach Profile Height
S_d	Water Depth at Submerged Beach Profile
CCD	Charge Coupled Device
WG	Wave Gauge

TABLE OF CONTENTS

LIST OF FIGURES

FIGURE Page

LIST OF TABLES

TABLE Page

1. INTRODUCTION

The Greater Houston Metropolitan Area (GHMA) was devastated after Hurricane Ike. Combining Ike's size and power with the coastal features of the GHMA created a large storm surge which flooded many areas along the coast, causing damage to infrastructure, dislodging thousands of people, and shutting down the local economy. The GHMA is a commercial and industrial power and has a population of almost 6.5 million according to projections by the US Census Bureau (USCB), which makes storm surge damage all the more costly, and all the more important to protect.

1.1 Hurricane Ike

Hurricane Ike made landfall in the United States along the Texas coast on September 13^{th} 2008. The large Category 2 hurricane hit the east end of the barrier island city of Galveston with 175 km/hr winds and 4.6 m (referenced from NAVD88) of storm surge before continuing on a direct path through Houston. [2]

Much of the damage caused by Ike was due to its high storm surge. Storm surge is a rise in sea level caused by heavy winds over a large area of ocean, blowing water towards the shore which raises the sea level along the coast. Ike's wind field was so large, 440 km radius at the time it made landfall, that it produced storm surge levels typical of Category 4 hurricanes [15] and caused sea levels all along the Gulf of Mexico (GoM) coast to rise above normal levels. On Galveston Island and Bolivar Peninsula, an estimated storm surge of 3 m to 4.6 m inundated portions of the low lying islands under more than 3 m of water. However, the highest storm surge was recorded just over eleven miles inland, at 5.3 m, due to the large surface area and shallow depth of Galveston Bay. [2]

Figure 1.1: Flooding on Galveston Island due to storm surge from Hurricane Ike. [2]

Coastal communities saw as many as 99% of homes inundated and over 60% completely destroyed by surge and large waves (see Figure 1.1). [15] The storm took twenty lives and cost an estimated $5 billion of property damage due to storm surge alone. Although Galveston currently has a seawall designed to protect against hurricane surge, the island was inundated from the bay side, as water flowed in through Bolivar Roads Pass, just beyond the existing seawall. (the total estimated value of property damage from Ike is $25 billion). [2]

1.2 Greater Houston Metropolitan Area

For the purposes of this thesis, the Greater Houston Metropolitan Area is defined as the coastal communities along Galveston Bay, which include Galveston, Harris and Chambers counties. This section looks at both natural and man-made characteristics of the area that make protecting the GHMA from storm surge a high priority.

1.2.1 Economic Value of the GHMA

The GHMA is the epicenter of the US oil and gas industry, which accounts for nearly 8% of the total US GDP [30] or almost $1.3 trillion, according to the US Department of Commerce's Bureau of Economic Analysis (BEA) [24]. Not only

is the area home to the US headquarters of the the world's energy industry, the GHMA has major contributions to production as well. The GHMA has nine crude oil refineries which, combined, account for just over 13% of the total US production. Petrochemical production in the GHMA is even greater, producing 38% of the US capacity [27, 28]. In total, the Gross Metropolitan Product (GMP) of the GHMA is roughly $450 billion in 2012 according to the BEA. [23]

Economic growth in the GHMA is also booming. Since 2002, the GHMA has experienced a 6.8% annual growth rate in GMP. Compared to the GDP annual growth rate at the national scale of 1.8% (calculated by averaging yearly values from The World Bank), the GHMA is greatly outpacing the national average. With roughly 6.5 million people, the GHMA ranks as the 5th largest metropolitan area in the United States. Not only is it one of the the largest, it is the US's third fastest growing metropolitan area. Figure 1.2 shows the trends for population and economic growth in the GHMA. [1, 5, 6, 22]

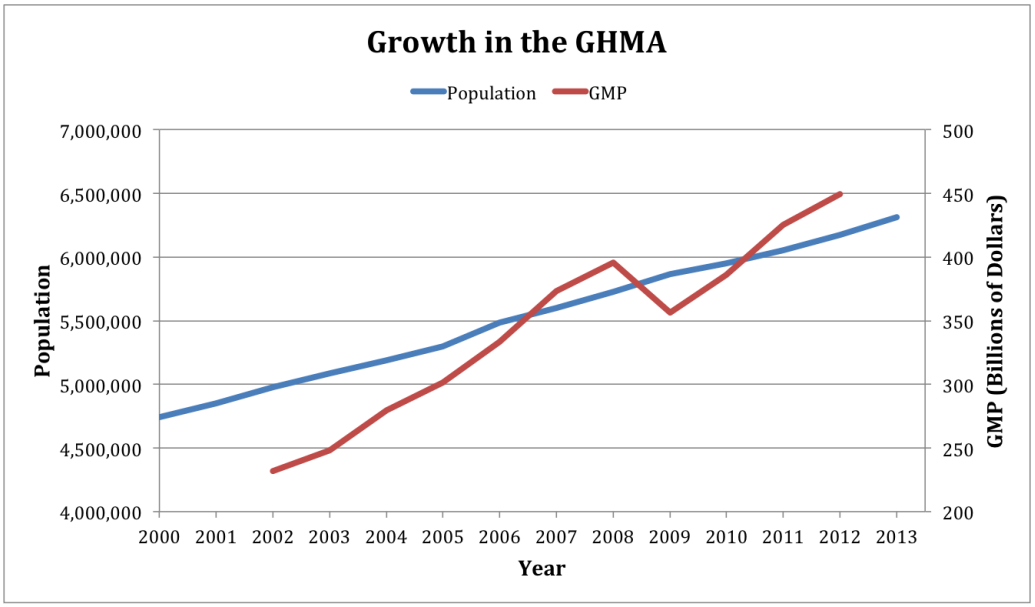

Figure 1.2: Population and Gross Metropolitan Product for the GHMA from 2000 to 2013. [4, 6, 23] The temporary decrease between 2007 and 2009 is a result of the nation-wide recession that caused a similar drop across the country.

1.2.2 Hurricane Surge Susceptibility

Two factors make the GHMA highly vulnerable to storm surge damage are the frequent occurrence of high surge events, and the flatness of the region's topography and bathymetry. With much of the GHMA's population and industry located in low-elevation areas, surge events pose a very dangerous risk.

Galveston Bay has a large surface area, approximately 1,400 km^2, and is very shallow for a body of water that size, with an average depth of only about 3 m. Furthermore, the flat topography surrounding the bay provides virtually no wind protection (see Figure 1.3). This combination creates the perfect conditions for storm surge. Similarly, the continental shelf along the Texas coast creates a large, shallow body of water with an average bottom slope of only 1v:2000h for almost 160 km offshore. Storm winds are free to blow unimpeded over the vast, shallow waters of the GHMA, causing exceptionally high surge elevations along the 480 km of coast and shoreline. [7, 10, 21, 29, 39]

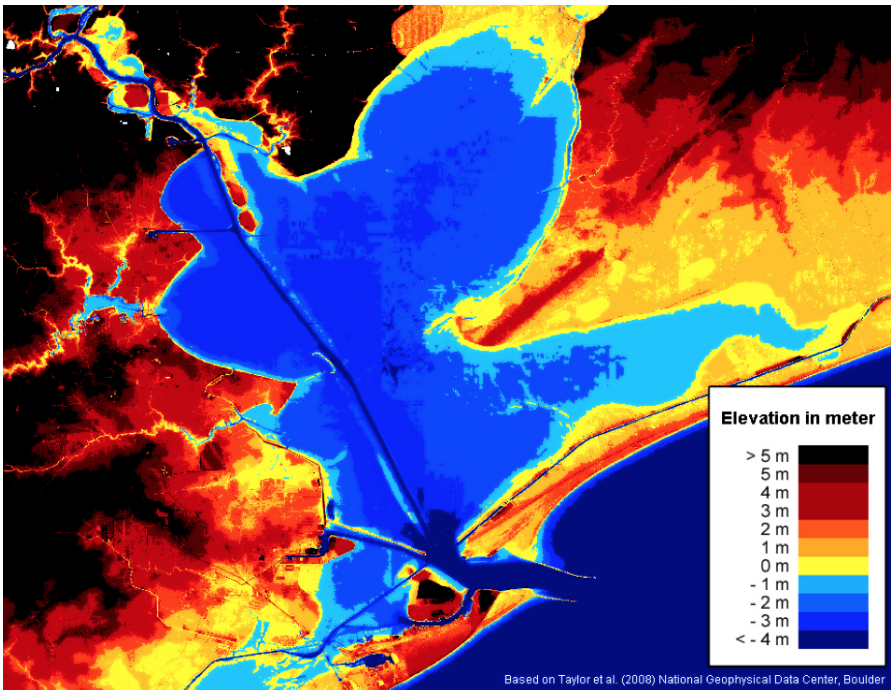

Figure 1.3: Elevation and topography of the GHMA measured from NAVD88. [41]

Tropical storms and hurricanes pose the greatest threat when it comes to storm surge in the GHMA. The storms have high enough winds to produce large surge and occur frequently in the area. Keim & Muller (2010) show that tropical storms that hit the GHMA have a return period of about 3 years, and hurricanes about 8 years (see Figure 1.4). While the strongest surge occurs directly where the storm makes landfall, storms that make landfall in close proximity can cause significant surge as well. Since 1900, 28 hurricanes have hit less than 200 km from Galveston. [16, 35]

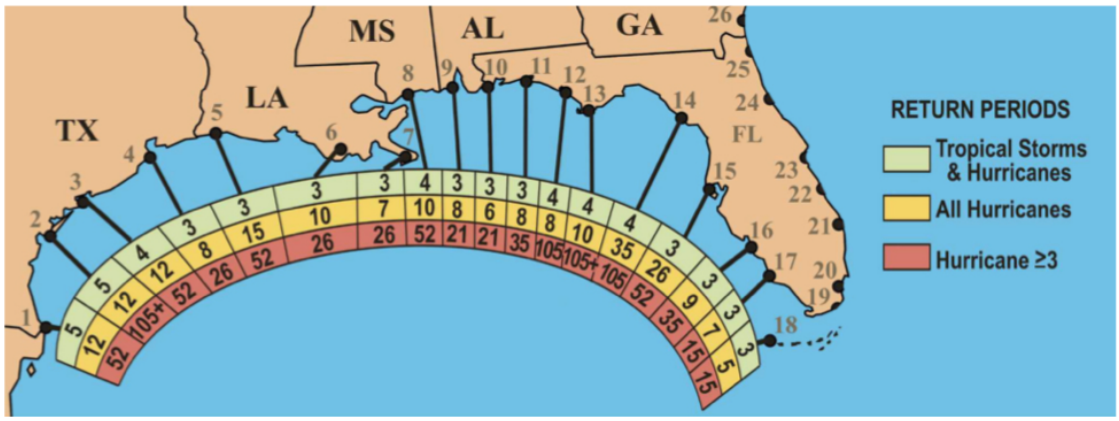

Figure 1.4: Return periods for tropical storms, hurricanes and major hurricanes hitting the US coast along the Gulf of Mexico (site 4 being the GHMA) [16]

1.3 The Netherlands and New Orleans

The Netherlands and New Orleans provide excellent case studies for implementing storm surge protection measures. Similar to the GHMA, both areas are highly susceptible to destructive surge flooding due to their low elevation and frequent surge events. In fact, both areas have large, populated regions that are entirely below sea level - effective ocean barriers are essential. These areas have implemented storm surge protection measures that have proven effective.

In 1953 the Netherlands was subjected to a natural catastrophe where over 1,800 people were killed due to flooding in the North Sea. The historically high flooding breached many of the existing levees and flooded highly populated areas. In response to this event, the Dutch government commissioned what has come to be known as

the Delta Committee. The committee was given the task of figuring out how the country could best prevent similar flooding events in the future. Instead of simply strengthening the existing levee system, the committee found that the best strategy would be to create a new system of levees that would shorten the barrier as much as possible (see Figure 1.5). Shortening the barrier creates a "coastal spine" that decreases the chance of failure as well as reduces cost, and is one of the key lessons learned from the Delta Works project. The barrier has been successful at preventing flood destruction since its construction. [38]

Figure 1.5: The Eastern Scheldt Storm Surge Barrier, part of the Delta Works, shows how the protective barrier was shortened by spanning an inlet. [17]

The New Orleans area faced similar destruction in 2005 when Hurricane Katrina, which reached Category 5 at its peak intensity, made landfall near the city. While not directly hit, the storm surge caused flooding that inflicted devastating damage to the region, due to the low lying (and partially below sea level) elevation of the city. In response, the Hurricane and Storm Damage Risk Reduction System (HSDRRS) Lake Borgne Surge Barrier was built to protect the area from future storm

surge flooding. The HSDRRS was conceived from a joint venture between the US Army Corps of Engineers (USACE) and the Netherlands, known as the Netherlands Water Partnership, in order to get a Dutch perspective given their expertise in surge protection. The result was that the HSDRRS was built with the same principles applied to the Delta Works half a century earlier, shortening the perimeter in order to create a unified defense with as little span as possible. [38]

1.4 The Ike Dike

After Hurricane Ike in 2008, Dr. William Merrell at Texas A&M University at Galveston looked to apply these lessons learned from the Netherlands and New Orleans to the GHMA. The result is what has come to be known as the Ike Dike. The Ike Dike would stretch 100 km along the Texas coast, and would protect not only Houston, but every city along Galveston Bay. To create the coastal spine, a levee system would both extend the protection granted by the Galveston Seawall to San Luis Pass as well as protect the Bolivar Peninsula from Bolivar Roads to Rollover Pass (see Figure 1.6). The levee system's proximity to the coast has not been established and early alternatives include raised highway levees and shoreline levees; the final design may include both features. The two sections of the proposed levee system will be connected by a barrier in the Bolivar Roads Pass which will allow for ship traffic and natural tidal flows when open, but could be closed quickly to form a solid protective barrier when dangerously high surge levels are predicted. [9, 20]

Figure 1.6: Aerial image showing the proposed layout of the Ike Dike levee system, with the existing Galveston Seawall highlighted in green. [9].

1.5 Objective

This thesis explores conceptual designs for the fixed barrier section of the proposed coastal spine, specifically focusing on a "Levee-in-Dune" concept. A Levee-in-Dune system was chosen because it can blend in, and even enhance, the natural landscape while providing the protection necessary to withstand a large hurricane. The channel barrier, connection to the channel barrier, and location of the levee system are beyond the scope of this investigation. Chapter 2 presents and analyzes four design alternatives based on cost and performance. A physical model of each design is tested in a two-dimensional flume under hurricane-like wave and surge conditions, described in Chapter 3. Finally, analysis of data collected during physical modeling is presented in Chapter 4 which allows for performance comparisons between the concepts as well as a better understanding of the underlying physical processes associated with dune erosion and structure interaction under hurricane conditions.

This work is meant to be a 'first cut' at evaluating various design alternatives for the Ike Dike en route to finding the best solution for protecting the people of Galveston, Chambers and Harris counties as well as the local and national economies from future shutdown due to hurricane flood damage. The findings that come from the design, evaluation, and testing presented in this thesis are meant to be the basis for the continuation and future direction of work on the Ike Dike project.

2. CONCEPTUAL DESIGNS

A Levee-in-Dune is a coastal barrier consisting of a protective levee core covered by a layer of sand that takes on the shape of a natural sand dune along a stretch of shoreline. In this initial design study for the fixed barrier portion of the Ike Dike, four Levee-in-Dune (LID) alternatives have been developed. The result is a set of design concepts that each create an aesthetically appealing stretch of LID's with a minimal environmental impact. The LID's natural sand dune appearance seamlessly blends in to the shoreline environment while providing additional habitat for coastal vegetation and fauna. The dune covers a protective core, which acts as an impermeable barrier during hurricanes, keeping storm surge from inundating the land behind it, as shown in Figure 2.1.

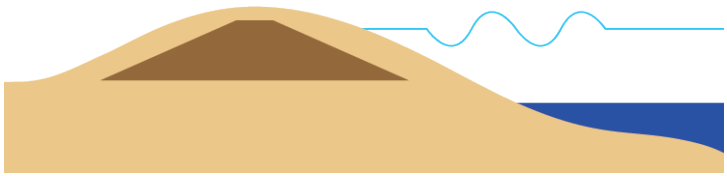

Figure 2.1: Basic cross-sectional diagram of an LID surge barrier.

The fixed barrier portion of the Ike Dike stretches roughly 85 km along Galveston Island and Bolivar Peninsula. In this initial concept evaluation phase it is assumed that the LID's will not need additional ramps, walkways or stairs. Future design refinement may include the use of such structures for ease of access, however the designs in this study will limit side slope such that they can be easily traversed by foot. The concepts presented in this study include a homogeneous sand dune with no additional core, and three dunes that each incorporate different protective cores: an armorstone revetment core, a clay levee core, and a concrete "T-Wall" core. This chapter presents preliminary designs of these concepts including cost estimations.

Already implemented in Noordwijk, South Holland, the Dutch levee-in-dune (dike in dune) has been an overall success. The *European Coastal & Marine Union*, a

renowned organization dedicated to bettering coastal communities throughout Europe by valuing sustainable development and social responsibility, praises the added value of Holland's LID:

> This innovative strategy has provided an array of benefits. The "dike in dune" has demonstrated to be an effective approach to provide sufficient protection against flooding and at the same time preserve the ecological, aesthetic and recreational values of the area. The integration of the dike into the dunes has helped to maintain the natural beauty of the dune landscape and it has provided new opportunities for recreation such as the path created on the new dunes, which has become an attractive site for tourists. Furthermore, this innovative solution has led to less restrictive planning and building regulations, providing more room for the future coastal development of the municipality.

2.1 General Core Design

Three of the four concepts presented in this thesis, excluding the T-Wall, employ an earthen levee design. Earthen levees are trapezoidal structures made of compacted soil and are commonly used for flood prevention along rivers and coasts. The design of earthen levees requires specification of fill material and four defining dimensions: height, crest width, front slope, and back slope, shown in Figure 2.2 and summarized in Table 2.1. These levee designs were based primarily on requirements and recommendations from the USACE's Engineering Manual 1110-2-1913, 'Design and Constructions of Levees'. [43]

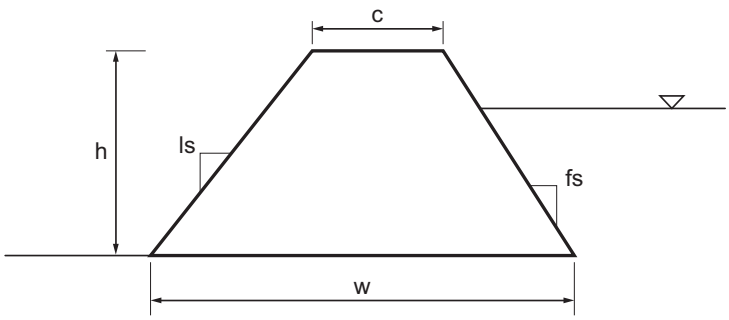

Figure 2.2: Cross-section of the general layout of an earthen levee with important design dimensions. h is the height of the levee, w is the footprint width, c is the crest width, fs is the flood-side slope and ls is the land-side slope.

The height of a levee has the most obvious impact on its effectiveness; the greater the height is, the higher surge level it can protect against. Common to all four concepts, the design height of the LID's protective core is fixed at 5.2 m, the height of the existing Galveston Seawall. This height affords the highest level of surge protection without having to raise the existing height of the seawall, a project that would be highly expensive and is presently not under consideration.

Like height, side slope specifications require careful consideration. Shallower slopes add stability while also serving to better dissipate wave energy and mitigate wave runup (flood-side), as well as reduce seepage through the structure (land-side). However, steeper slopes allow for a more compact design, requiring less material and leaving a smaller footprint. Guidance from the USACE limits side slope to a maximum of 1v:2h, but also indicates that a 1v:3h slope is recommended in order for the levee to be easily traversed. To allow for convenient beach access by foot, the 1v:3h slope was chosen as the maximum slope (flood- or land-side) for any concept.

The determination of crest width may be driven by a levee's secondary functionality, such as a levee-top road. Since these initial concepts do not call for such auxiliary functions, the crest width was selected to the USACE's minimum required crest width of 3 m for all LID designs. This requirement exists for construction and maintenance purposes.

To create a more natural and aesthetically appealing look, a layer of sand enshrouding the protective core was added to the design. However, the sand layer has

functional purposes as well. The sand layer provides a sufficient foothold for dune vegetation to develop a strong root system and also acts as a barrier between beach-goers and the core structure. Additionally, the sand layer can act as "sacrificial" material during storm events, taking the brunt of the storm and eroding away before the protective core is ever exposed. Since design parameters for a protective sand layer have not been developed, a thickness of 1 m (about 20 % of the core height) was chosen for the initial design study. This value, though somewhat arbitrary is considered a reasonable starting point, however further refinement is necessary in future considerations. Overwash, when the wave height exceeds the height of the dune, is a critical factor which may drive the sand layer to increase in thickness. However, the present dune height was designed so that no overwash is anticipated.

Table 2.1: Design parameters common to all four LID concepts.

Core Height	Side Slope Limit	Crest Width	Sand Layer Thickness
5.2 m	1h:3v	3 m	1 m

2.2 Sand Dune

The first and most basic design considered is a sand dune with no additional core material, referred to as the "No-Core" LID concept. For the purpose of better comparison in the initial design phase, the dimensions and shape of the No-Core concept were determined by designing a theoretical sand "levee" core and then adding a layer of sand to cover the core, as would be the case in designs with separate cores. In reality, there is no distinction between the sand core and the sand cover layer. Although intended mostly as a baseline for comparison purposes for the dune-structure interaction associated with the other LID concepts, it is not ruled out as an option and its performance is considered.

Under high surge and large wave attack, sand from the flood-side of the No-Core LID will erode away with rapid cross-shore transport. Much of this section of the dune and levee will act as sacrificial material, with enough remaining dune structure to outlast the storm and protect the area behind it. Some of the sacrificial material will settle just offshore, changing the submerged beach profile, which will act to

dissipate wave energy from directly hitting the dune. The larger waves will break farther offshore while passing over the altered submerged profile, dissipating much of the wave's energy into fluid turbulence instead of sediment transport.

With the levee height, flood-side slope and crest width determined, the only remaining dimension is the back side slope. The maximum slope considered is 1v:3h in order for beach-goers to easily walk over the dune, however the USACE adds an additional constraint on sand levees due to their high porosity which makes them susceptible to seepage. Sand levees must have a land-side slope of at most 1v:5h, which is the value chosen for the No-Core LID. This requirement adds a considerable volume and footprint width to the concept. The sand layer follows the contour of the levee, keeping a constant vertical thickness of 1 m. A diagram of the No-Core LID is shown in Figure 2.3.

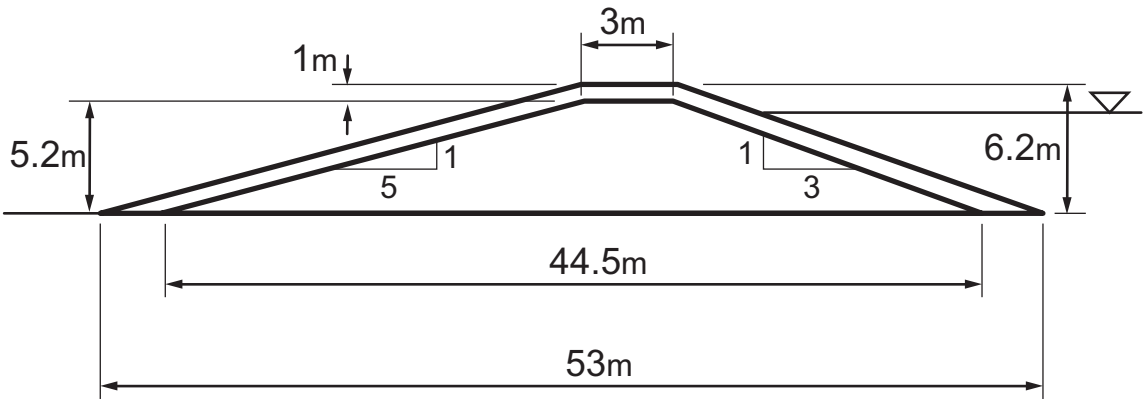

Figure 2.3: Cross-sectional schematic of the No-Core LID concept.

No-Core LID design summary:

- Height 5.2 m (Seawall constraint)
- Flood-side slope 1v:3h (USACE recommended slope)
- Land-side slope 1:v5h (USACE required back slope for sand levee)
- Crest width 3 m (USACE minimum)

- Sand layer $\underline{1\,\text{m}}$ (20% of levee height)

The volume of sand required for the No-Core LID can be estimated by assuming a perfectly trapezoidal shape. In reality, the upper vertices of the levee will be rounded, and the lower verticies will taper to converge with the natural beach profile, rather than coming to sharp points. However, the trapezoid is a good estimate for the volume of sand required for the concept. The equation for the volume of the trapezoid formed by the LID is:

$$\frac{V_s}{L} = \frac{1}{2}(c + w)h_d \tag{2.1}$$

$\frac{V_s}{L}$, c, w, and h_d are sand volume per unit length, crest width, footprint width, and dune height, respectively. The angles of the flood-side and land-side slopes (from horizontal) are θ_{flood} and θ_{land}, respectively. To find footprint width:

$$w = c + h_d \arctan(\theta_{flood}) + h_d \arctan(\theta_{land}) \tag{2.2}$$

$$w = 3\,\text{m} + 6.2\,\text{m}(5 + 3) = 53\,\text{m}$$

Solving for volume,

$$\frac{V_s}{L} = \frac{1}{2}(3\,\text{m} + 53\,\text{m})6.2\,\text{m} = 175\,{}^{\text{m}^3}/_{\text{m}}$$

2.3 Armorstone Revetment Levee

The "Armorstone-Core" LID concept is virtually identical to the No-Core LID, with the addition of an armorstone revetment buried under the sand layer. The two-layer, uniform quarystone revetment is placed along the leading face and crest of the sand levee. Revetments are a common solution for coastal engineers trying to mitigate shoreline erosion from wave attack; a similar revetment core was used when the Netherlands built the 'dike in dune' in Noordwijk, as mentioned in the introduction of this chapter. The large stones dissipate wave energy and reduce runup, helping protect the core sediment from being washed away. A diagram of the Armorstone-Core LID is shown in Figure 2.4.

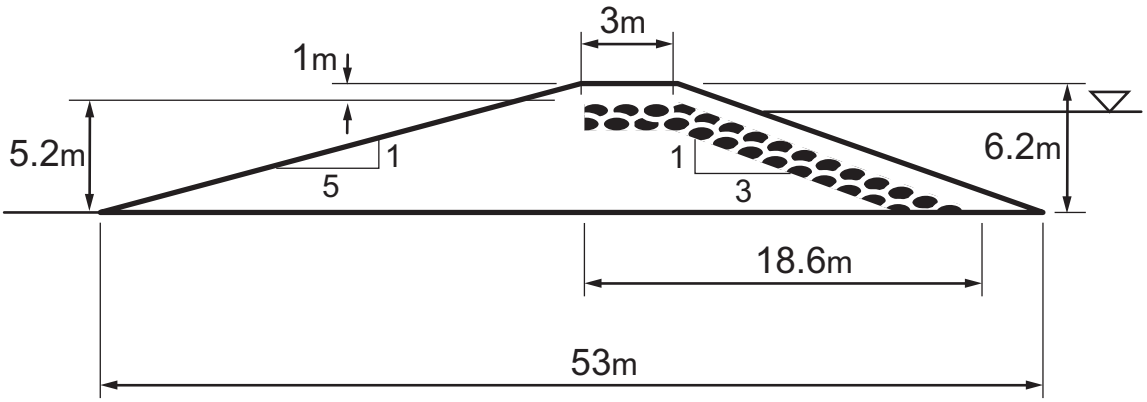

Figure 2.4: Cross-sectional schematic of the Armorstone-Core LID concept.

The armorstone units must be large enough to stay in place during storm conditions, and in order to properly size them, Hudson's Equation (Eq. 2.3) is used. Hudson's equation was developed by the USACE and is commonly used to size riprap for revetments subject to large wave attack. For rock sizing, the 100-year return period significant wave height, 2.4 m, is used. [39, 44]

Following Hudson's Equation:

$$M_{50} = \frac{\rho_r H^3}{K_D (S_r - 1)^3 \cot\theta} \tag{2.3}$$

Where M_{50}, ρ_r, H, K_D, S_r, and θ are the median stone mass, density of the stone, design wave height, stability coefficient, relative density of stone to water, and flood-side slope of the revetment. Values are taken from the US Department of Transportation. [45]

$$M_{50} = \frac{(2,650\,{}^{kg}/_{\mathrm{m}^3})(2.4\,\mathrm{m})^3}{(2.2)(2.4-1)^3(3)} = \underline{2023\,\mathrm{kg}}$$

Converting to diameter, assuming a spherical stone unit:

$$D_{50} = (1.27)\sqrt[3]{\frac{M_{50}}{\rho_r}} = \underline{1.2\,\mathrm{m}} \tag{2.4}$$

Armorstone-Core LID design summary:

- Height $\underline{5.2\,\mathrm{m}}$ (Seawall constraint)

- Armorstone $\underline{D_{50}\ 1.2\,\mathrm{m}}$ (Hudson's Equation)
- Flood-side slope $\underline{1\text{v:}3\text{h}}$ (USACE recommended slope)
- Land-side slope $\underline{1\text{:v}5\text{h}}$ (USACE required back slope for sand levee)
- Crest width $\underline{3\,\mathrm{m}}$ (USACE minimum)
- Sand layer $\underline{1\,\mathrm{m}}$ (20% of levee height)

The Armorstone-Core LID uses only sand and quarrystone. To determine the volume of quarrystone required, the average thickness and porosity of the two armorstone layers must be found. The average thickness can be found by the following equation:

$$r = nk_{\Delta}(\frac{M_{50}}{\rho_r})^{1/3} \tag{2.5}$$

Here r, n, k_{Δ} represent the average thickness of the armorstone layer, number of layers, and layer coefficient, respectively. This equation and its values are taken from the Coastal Engineering Manual. [44]

$$r = (2)(1)(\frac{2,023\,\mathrm{kg}}{2,650\,{}^{kg}/_{\mathrm{m}^3}})^{1/3} = \underline{1.8\,\mathrm{m}}$$

The Armorstone-Core LID cross-section has 18.6 m of armorstone, bringing the total volume per unit length of the armorstone (assuming porosity, $n_a = 0.45$) [31] to be:

$$\frac{V_{armorstone}}{L} = (18.6\,\mathrm{m})(1.8\,\mathrm{m})(0.45) = 15.3\,{}^{\mathrm{m}^3}/_{\mathrm{m}}$$

To estimate the amount of material required, the same trapezoidal shape assumptions are used as for the sand dune. Since the shape of the dune is identical to the No-Core LID, the core volume is subtracted from the sand volume required for the No-Core LID to find the sand volume for this concept.

$$\frac{V_s}{L} = \frac{V_{s,no-core}}{L} - \frac{V_{armorstone}}{L} \tag{2.6}$$

$$\frac{V_s}{L} = 175\,{}^{\mathrm{m}^3}/_{\mathrm{m}} - 15.3\,{}^{\mathrm{m}^3}/_{\mathrm{m}} = \underline{159.7\,{}^{\mathrm{m}^3}/_{\mathrm{m}}}$$

2.4 Clay Levee

One of the problems with a sand levee is its high porosity. The high porosity is the reason for the long flood-side slope, which greatly increases the overall footprint of the LID as well as the material necessary to construct it. In order to shorten the dune, a less porous core material such as clay must be used. A common levee fill material, clay offers a variety of benefits over sand. Clay not only has lower porosity, with hydraulic conductivity rates up to seven orders of magnitude smaller than sand, making seepage a non-issue, it is also a cohesive soil with much greater shear strength than sand. Furthermore, clay is abundantly available in Eastern Texas. These are just a few of the properties that make clay an ideal material for a protective levee core. [11]

Clay's advantageous soil properties allow for the dimensions of the dune to be substantially reduced. The "Clay-Core" LID does not require the 1v:5h land-side slope and can be reduced to 1v:3h. All other dimensions remain the same as the No-Core and Armorstone-Core LID concepts. A diagram of the Clay-Core LID is shown in Figure 2.5.

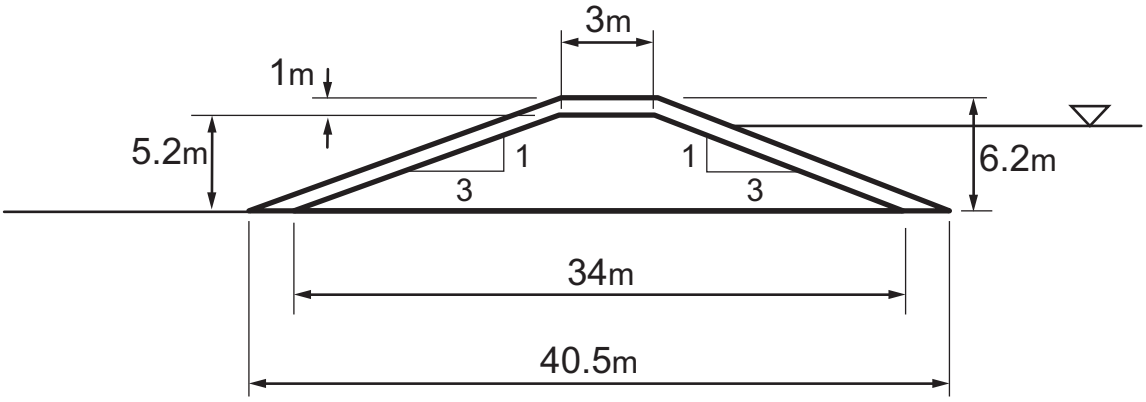

Figure 2.5: Cross-sectional schematic of the Clay-Core LID concept.

Clay-Core LID design summary:

- Height 5.2 m (Seawall constraint)

- Flood-side slope 1v:3h (USACE recommended slope)
- Land-side slope 1:v3h (USACE recommended slope)
- Crest width 3 m (USACE minimum)
- Sand layer 1 m (20% of levee height)

To estimate the amount of sand and clay needed for the Clay-Core LID, a trapezoidal assumption for both the clay core and the total LID volume is used. To find the amount of sand required, the core volume is subtracted from the total volume.

$$\frac{V_s}{L} = \frac{V_{LID}}{L} - \frac{V_c}{L} \tag{2.7}$$

First solve for total LID volume:

$$\frac{V_{LID}}{L} = \frac{1}{2}(c + w_d)h_d \tag{2.8}$$

$$w_d = c + h_d \arctan(\theta_{flood}) + h_d \arctan(\theta_{land}) \tag{2.9}$$

$$w_d = 3\,\text{m} + 6.2\,\text{m}(3+3) = 40.5\,\text{m}$$

Solving for volume,

$$\frac{V_{LID}}{L} = \frac{1}{2}(3\,\text{m} + 40.5\,\text{m})6.2\,\text{m} = 135.5\,\text{m}^3/\text{m}$$

Next, core volume is determined:

$$\frac{V_c}{L} = \frac{1}{2}(c + w_l)h_l \tag{2.10}$$

$$w_l = c + h_l \arctan(\theta_{flood}) + h_l \arctan(\theta_{land}) \tag{2.11}$$

$$w_l = 3\,\text{m} + 5.2\,\text{m}(3+3) = 34.1\,\text{m}$$

Solving for volume,

$$\frac{V_c}{L} = \frac{1}{2}(3\,\text{m} + 34.1\,\text{m})5.2\,\text{m} = 96.3\,\text{m}^3/\text{m}$$

Finally, solving for sand volume:

$$\frac{V_s}{L} = 135.5\,\text{m}^3/\text{m} - 96.3\,\text{m}^3/\text{m} = \underline{39.2\,\text{m}^3/\text{m}}$$

2.5 T-Wall Levee

One of the primary failure modes of the levee system in New Orleans during Hurricane Katrina was "I-Wall" toppling. An I-Wall is simply a vertical metal or concrete wall buried deep in order to be able to withstand some storm surge. The I-Wall design was used throughout the old levee system, but was not strong enough to withstand the high surges generated by Katrina. Scour caused by overtopping eroded the soil that held the walls in place, leading to the wall's collapse and massive destruction. Learning from these failures, the new HSDRRS barrier eliminated the use of I-Walls and extensively incorporated much more robust T-Walls. The enthusiastic use of T-Walls inspired their inclusion among the preliminary designs for the Ike Dike coastal spine.

The T-Wall is an impermeable concrete barrier with a wide base and long steel piles that help prevent toppling when subject to extreme hydrostatic pressure caused by large surge (see Figure 2.6). Water pressure along the long toe of the wall creates a restoring moment to counteract the pressure along the vertical portion of the wall, keeping it upright. Sheet piling underneath the center of the wall keeps water from seeping directly under the wall.

For this study, the design of the T-Wall concept is based on an example design provided by the USACE. The example design uses the same design height, 5.2 m, as the existing seawall and proposed Ike Dike design height. However, the example uses a surge height of 5.2 m and stands alone without a dune cover, making the example a "worst case" load condition. This will be a good starting point for the design, conservative enough to handle the worst load possible, yet realistic to the design conditions. To complete the LID design, the sand layer is added, with both flood-side and land-side slopes of 1v:3h. The placement of the T-Wall within the dune is such that the leading edge of the wall is aligned with the flood-side upper vertex of the dune. [46, 47] A diagram of the T-Wall LID is shown in Figure 2.7.

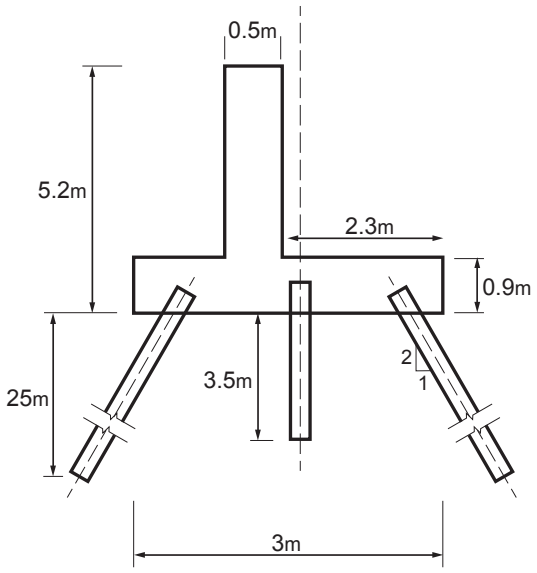

Figure 2.6: Cross-sectional schematic of the T-Wall core structure for the T-Wall LID concept.

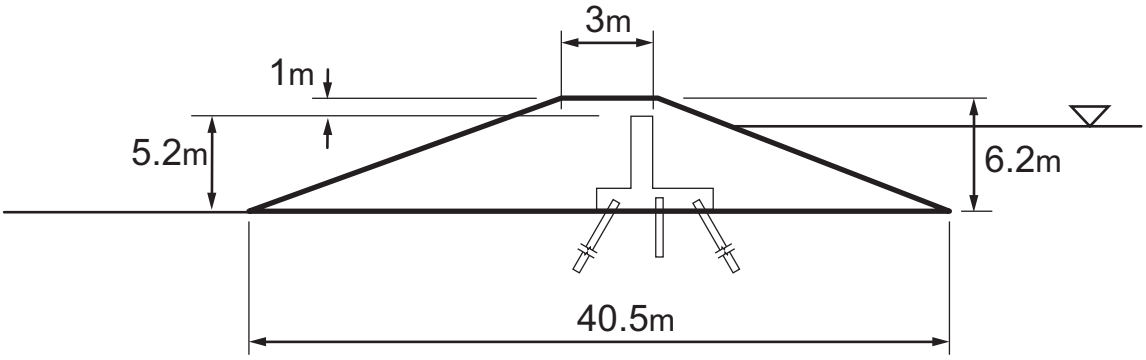

Figure 2.7: Cross-sectional schematic of the T-Wall LID concept.

T-Wall LID design summary:

- Height 5.2 m (Seawall constraint)
- Wall Thickness 0.5 m (USACE example)

- Base Width $\underline{3\,\text{m}}$ (USACE example)
- Base Thickness $\underline{0.9\,\text{m}}$ (USACE example)
- Flood-side dune slope $\underline{1\text{v:}3\text{h}}$ (USACE recommended slope)
- Land-side dune slope $\underline{1\text{:v}3\text{h}}$ (USACE recommended slope)
- Crest width $\underline{3\,\text{m}}$ (USACE minimum)
- Sand layer $\underline{1\,\text{m}}$ (20% of levee height)

To determine the volume of sand required for the T-Wall, the dune is once again assumed to be a trapezoid. The volume of the wall is then calculated:

$$\frac{V_W}{L} = wt_b + (h - t_b)t_v \tag{2.12}$$

Where t_b and t_v are the thicknesses of the base and vertical portion of the T-Wall, and w is the width of the base.

$$\frac{V_W}{L} = (3\,\text{m})(0.9\,\text{m}) + (5.2\,\text{m} - 0.9\,\text{m})(0.5\,\text{m}) = 4.7\,{}^{\text{m}^3}/_{\text{m}}$$

Since the T-Wall-Core LID has the same dune shape as the Clay-Core LID, the previously calculated total dune volume is used and the T-Wall volume subtracted out.

$$\frac{V_s}{L} = \frac{V_{LID}}{L} - \frac{V_W}{L} = 135.5\,{}^{\text{m}^3}/_{\text{m}} - 4.7\,{}^{\text{m}^3}/_{\text{m}} = \underline{130.8\,{}^{\text{m}^3}/_{\text{m}}}$$

2.6 Natural Dune Erosion

Natural sand dunes provide a line of defense against flooding and wave damage during storms. As a "soft" structure, sand dunes are subject to change over the course of a storm. They act as a sacrificial barrier, wave energy dissipated into the dune initiates and drives sediment transport away from the dune, slowly eroding away. Dunes experience three types of erosion: scarping, overwash and inundation [40]. Scarping occurs when the water level is low enough so that no overtopping occurs, and waves slowly wash away the face of the dune. Overwash occurs when enough overtopping occurs to weaken the dunes where they are shortest, causing a local breach (see Figure 2.8). Inundation occurs when the water level exceeds the height

of the dune, submerging nearly the entire area behind the barrier and completely destroying the dune. [26]. The physical modeling portion of this thesis focuses on scarping erosion, since no overtopping is considered.

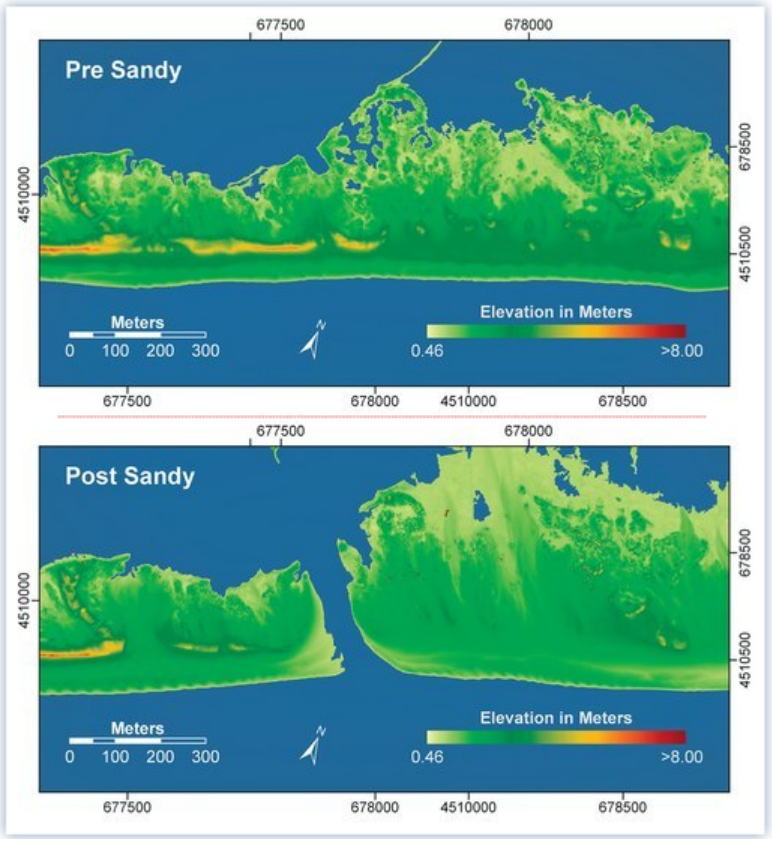

Figure 2.8: Aerial view of Fire Island, NY showing overwash damage caused by hurricane Sandy. [34]

2.7 Rough Cost Estimate

While reports on project costs are scarce and what little information is available is usually a relatively poor predictor based on substantial differences between projects, Hoozemans et al. have established rough estimates for the cost of different types of coastal levees [13, 38]. The study finds that the rough cost for artificial sand dunes is \$6.1 M per km, stone-protected levees is \$6.1 M - \$11.5 M per km, and clay levees

is \$3.4 M per km. In another study, the California Delta Vision estimates the cost of an earthen levee to be \$5.7 M per km, which agrees with Hoozemans [3]. After Katrina, 37 km of T-Wall levees were built along St. Bernard Parish, costing \$1.25B, bringing the cost of the T-Wall levees to be \$33.5 M per km [25]. This is likely more than the cost of the T-Wall within the LID since the St. Bernard walls are larger, providing a conservative estimate.

2.8 Design Summary

Designs for all four LID concepts (No-Core, Armorstone-Core, Clay-Core and T-Wall) are summarized in Tables 2.2 - 2.4. Table 2.2 lists the defining dimensions common to all LID concepts and Tables 2.3 and 2.4 list the "per km" and total material and cost requirements of each design, respectively. Table 2.5 presents perceived design advantages and disadvantages for each concept. A "+" is given to the concept with the most desirable value in a category and a "-" is given to the concept with the least desirable value.

Table 2.2: Important design parameters for each LID concept.

Concept	No Core	Armorstone	Clay	T-Wall
Height [m]	5.2	5.2	5.2	5.2
Sand Layer Thickness [m]	1	1	1	1
Crest Width [m]	3	3	3	3
Total Footprint Width [m]	53	53	40.5	40.5
Flood-Side Slope [-]	1v:3h	1v:3h	1v:3h	1v:3h
Land-Side Slope [-]	1v:5h	1v:5h	1v:3h	1v:3h

Table 2.3: Required volume of all LID materials per meter of dune (km for cost).

Concept	No Core	Armorstone	Clay	T-Wall
Sand Volume [$^{m^3}/_{m}$]	174.3	159	39.2	130.8
Core Volume [$^{m^3}/_{m}$]	-	15.3	96.3	4.7
Total Volume [$^{m^3}/_{m}$]	174.3	174.3	135.5	135.5
Cost [$^{\$M}/_{km}$]	5.7-6.1	6.1-11.5	3.4-5.7	33.6

Table 2.4: Total required volume of all LID materials, based on 83 km of added LID.

Concept	No Core	Armorstone	Clay	T-Wall
Sand Volume [Mm^3]	14.6	13.3	3.3	10.9
Core Volume [Mm^3]	-	1.3	8.0	0.4
Total Volume [Mm^3]	14.6	14.6	11.3	11.3
Cost [$M]	473-510	510-962	286-473	2,808

Table 2.5: Summary table of perceived advantages and disadvantages of each LID concept. Advantages are marked with a '+', disadvantages with a '-', and neutral categories left blank.

Concept	No Core	Armorstone	Clay	T-Wall
Footprint	-	-	+	+
Durability	-			+
Cost			+	-

3. PHYSICAL MODELING

This chapter describes the experiment setup, instrumentation including calibration, and procedure used for modeling the LID concepts in the Coastal Processes Flume (CPF) at Texas A&M University at Galveston (TAMUG).

Physical experiments involving evolving beach profiles inherently prove challenging due to the complex interlinked processes and feedback mechanisms of hydrodynamic forcing and bottom morphology. The addition of hard structures buried under the beach profile only adds further complication, and the resulting effects on morphology and erosion are virtually unknown. Understanding how the presence of sand-covered hard structures affects the morphology of beach profiles during storm events is crucial for the design of a coastal surge barrier.

3.1 Experiment Setup

Physical modeling of the four LID concepts was performed in the CPF at TAMUG. The CPF measures 15 m long, 1.2 m deep and 0.6 m wide as shown in Figure 3.1. Regular and spectral waves are capable of being generated by the flume's flap-style wavemaker, which is controlled by LabView. The experiment makes use of a cache of wave gauges to measure free surface elevation at various points along the flume. A rail system above the flume allows an instrument-carrying cart to move in the cross-shore direction, allowing measurements to be taken along the profile.

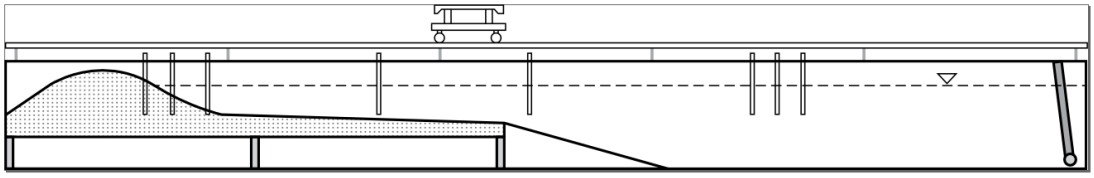

Figure 3.1: Schematic of Coastal Processes Flume at Texas A&M Galveston.

The flume has a wooden frame that supports a sandy beach. The wavemaker requires that the flume maintains a minimum water depth of roughly 70 cm in order to operate smoothly. The 45 cm tall frame gives the beach a boost in height which

allows for a higher water level while reducing the amount of sand required to construct an appropriate dune.

3.1.1 Model

The model for the physical experiment was built at a scale of 1:18 (s_m) of full size. This is the largest scale factor achievable given the physical constraints of the flume and wave maker. It is important to have the largest scale practicable in order to preserve relevant physical phenomena. At small scale, sandy sediments can become cohesive, which dramatically changes the nature of sediment transport. Typical scale factors used for physical models in coastal engineering range from 1:10 to 1:100. [10]

The model has 8 m of beach at a slope of 1v:50h preceding the dune, chosen as a representative nearshore beach slope from analysis of survey data taken on Galveston Island preceding Hurricane Ike. [19] The base of the dune is constructed at an elevation corresponding to MSL. The model dune was constructed with a landward slope of 1v:2h to allow the dune to be placed further down the flume. This change does affect seepage through the dune, however does not affect erosion during storm testing which is the phenomenon of interest in this experiment. The ability to construct a longer, more realistic beach profile leading to the dune outweighs the higher risk of seepage on the landward side of the dune. Table 3.1 presents dune height and width ($H_{D,m}$, $w_{d,m}$), levee height ($h_{l,m}$) and sand layer thickness (t_m) at model scale.

Table 3.1: Model dune and levee dimensions.

$h_{d,m}$	$w_{d,m}$	$h_{l,m}$	t_m
35 cm	212 cm	29 cm	6 cm

3.1.2 Hydrodynamic Conditions

The hydrodynamic conditions for testing the LID configurations were chosen so that damage to the LID that would expose the underlying core in order to allow for a comparison between concepts. The initial estimate for choosing storm conditions was based on the 100-year storm for the area. 100-year return values for surge level (h_s), significant wave height (H_s) and peak wave period (T_p) were used as

parameters to mimic the environmental conditions of a storm that has a 1% chance of making landfall near the GHMA in any given year, Table 3.2 lists these values. [39] A JONSWAP spectrum using scaled values of H_s and T_p is used to create a realistic wave climate.

Once determined, the values were converted to model scale for the wave flume. Wave height and water depth were scaled geometrically by the same factor as the dune, s_m. In order to keep the model undistorted, the wavelength was also scaled by s_m. Keeping the wave undistorted constrains the model's peak period ($T_{p,m}$), which can then easily be solved for using the dispersion relation: [10]

$$T_p = \frac{2\pi}{\sqrt{gk \tanh(kh)}} \tag{3.1}$$

The dispersion relation is first used to solve for the full-scale wavenumber (k), based on measured wave period. Here, h is the water depth where the waves were recorded and g represents the Earth's gravitational acceleration. Given the form of the equation, it is impossible to solve for k analytically, so numerical methods must be used. The wavenumber can then be scaled to its model value where once again the dispersion relation is used to solve for the spectral peak period for the model:

$$T_{p,m} = \frac{2\pi}{\sqrt{gk_m \tanh(k_m h_m)}} \tag{3.2}$$

Here, the subscript m denotes "at model scale". Table 3.2 lists all relevant hydrodynamic conditions at both full and model scale.

Table 3.2: Hydrodynamic conditions starting with the 100-year return period storm for Galveston, TX at both full and model scale as well as final experiment inputs. [9]

Scale	h [39]	H_s [12, 14]	T_p [14]	λ_p
Full	3.9 m	2.4 m	6.6 s	42.7 m
Model [1/18]	21.7 cm	13.3 cm	1.24 s	237 cm
Final Experimental Values	21.7 cm	8.0 cm	1.1 s	189 cm

A series of test wave bursts were run in order to check the amount of erosion

caused by the scaled 100-year storm. For the experiment, it was desired that the wave bursts should expose the LID core, but gradually enough in order to be able to determine the effect of each LID. Initially, the dune was destroyed too rapidly so the values of H_s and T_p were adjusted until the desired amount of erosion occurred. In order to expose the core without completely destroying the dune, the significant wave height and peak spectral period were reduced to values shown in Table 3.2.

3.1.3 Core and Sediment Characteristics

Each LID requires a unique material to construct. In addition to sand, the Clay-Core LID is made from locally sourced "Campeche" clay, the Armorstone-Core LID is comprised of model-scale rocks, and the T-Wall LID uses plywood to simulate concrete at model scale.

The flume is filled with sand which has a median diameter of 0.14 mm as analyzed by a Malvern Mastersizer 2000E particle size analyzer. This fine-grained sand is representative of sand found in the Galveston area, which was analyzed and found to have a median grain size of 0.17 mm. [42] The grain size of the sand cannot be scaled in the same way that the dune dimensions can be scaled. A sediment with a grain size of the required scaled diameter (0.0094 mm) is classified as a silt rather than sand and becomes cohesive, altering its physical behavior. A cohesive sediment binds together, making it much more difficult to suspend than non-cohesive sediment at similar grain sizes. [10]

The Campeche clay used to make the Clay-Core LID was taken from a local area approximately 20 miles inland of Galveston in Santa Fe, Texas. The sticky clay was tested for basic soil properties including plastic limit, liquid limit and compression strength. The results are highlighted in Table 3.3, and the full method of calculation can be found in Appendix A.

Table 3.3: Soil parameters of the Campeche Clay used to construct the Clay-Core LID. Note that moisture content for unconfined compression strength was 0%.

Liquid Limit	Plastic Limit	Plasticity Index	Shear Strength
59 %	25%	34%	$46^{lbs}/_{in^2}$

The rock sizing for the armorstone layer in the Armorstone-Core LID was based on the Hudson Equation (Eq 2.3), just as the sizing for the full-scale design was done, using model-scale hydrodynamic conditions.

$$M_{50} = \frac{(2650\,{}^{kg}/_{\mathrm{m}^3})(0.13\,\mathrm{m})^3}{(2.2)((1.4)-1)^3(3)} = 0.4\,\mathrm{kg}$$

$$D_{50} = 1.27\sqrt[3]{\frac{0.4\,\mathrm{kg}}{2650\,{}^{kg}/_{\mathrm{m}^3}}} = 0.065\,\mathrm{m}$$

With the size of the model armorstone units being just 6.5 cm, it was possible to use landscaping rocks with a very similar gradation. The landscaping rocks were angular to subrounded in shape, which creates similar interlocking to what is expected in the full-sized design. Two layers of rock were placed by hand 5 cm along the front face and crest of the levee and then covered with a layer of sand. In order to replicate this at full-scale, each rock would be placed individually by crane to ensure a tight pack.

The T-Wall LID model used a plywood T-Wall made of $\frac{5}{8}$ in thick sheets. The plywood was cut to the appropriate height and base width, however the thickness was not to scale. A scaled thickness would be 1 in for the vertical face and 2 in for the base. However, the most important aspect to represent with the T-Wall LID is the solid, impermeable wall that stays in place under the experimental wave loads. The thinner plywood was adequate in that respect and therefore deemed appropriate for testing the T-Wall LID concept. The T-Wall was then buried so that the front edge of the vertical face was directly under the top-front vertex of the dune and the top was covered in 5 cm of sand.

3.2 Instrumentation and Measurement

The main phenomenon being measured in this experiment is dune morphology, which is primarily driven by wave forcing. It is therefore important to be able to generate precise and consistent waves, and accurately measure waves and beach profile change.

3.2.1 Waves

Wave bursts are generated by a 'flap-style' wavemaker, located at the far end of the flume. A LabView program controls the wave generating output signal while recording wave gauge data through a National Instruments data acquisition board.

The wave output signal and the wave gauge data run at 20 Hz, producing a Nyquist Frequency of 10 Hz, and the 280 s time series corresponds to a fundamental frequency of 0.0036 Hz. The peak frequency of the JONSWAP spectral input is 0.91 Hz, which falls well between the two limits.

The LID experiment utilized a cache of eight RBR WG-55 capacitance-style wave gauges to measure wave profiles at various locations. Gauges were placed such that they are approximately along the centerline of the flume to avoid wall effects. Three gauges are located in the deep water portion of the flume and spaced to best separate incident and reflected wave spectra according to Mansard and Funke (1980) [18]. The remaining five gauges are spaced throughout the sloping beach to view wave transformation from deep water to wave breaking, with a heavier concentration placed near wave breaking to more carefully observe inner surf-zone dynamics and wave up-rush. As the beach becomes shallower, the physical limitations of installing the wave gauges force some of the wave gauges to be partially buried in order to capture hydrodynamic effects of dune erosion. For the Clay-Core LID and Armorstone-Core LID, WG8 was removed due to interference with the core. Table 3.4 shows the location and initial condition of each wave gauge.

Table 3.4: Wave gauge locations. x-positions are taken as distance from wavemaker.

Gauge	WG1	WG2	WG3	WG4	WG5	WG6	WG7	WG8
x-position (m)	0.0	0.24	0.59	2.91	5.91	10.31	10.81	11.21
Initially Buried	No	No	No	No	No	Yes	Yes	Yes

Calibrating the wave gauges requires taking measurements at known water level increments in order to generate a voltage versus depth plot. The capacitance-style wave gauges comprise of a vertically aligned wire loop and frequency oscillators. Submerging the wire loop creates a certain capacitance in the loop that is then translated into a voltage. By capturing multiple known depths, a calibration curve can be calculated for converting voltage readings into wave height. [33]

3.2.2 Profiling

Obtaining high resolution profile changes is necessary to accurately observe morphology over time. For this experiment, a Class 3B Acuity AP820-1000 laser scanner was used to measure changes in the beach profile. The AP820 takes longshore 'slices' within its vertical operating range of 1.5 m - 0.5 m. A beam of 450 nm visible laser light projects a blue line on the target surface, which is detected from an angle by a two-dimensional charge coupled device (CCD) detector array. A 2D contour profile is then made by the scanner's signal processor using optical triangulation. [36, 37]

The laser scanner is mounted on a frame that moves on a track above the flume, allowing the laser to take measurements along the profile at numerous cross-shore locations while maintaining a consistent height. The frame is constructed such that the entire dune and beach profile fall within the laser's operating range. The AP820 works well even on reflective surfaces, which is important as most scans were taken over wet sand. Software provided by Acuity was used for data acquisition.

3.3 Procedure

The following steps outline the experimental procedure used for each test of the LID concept physical modeling.

1. **Create Levee-in-Dune** - The first step during testing is to construct the levee according to its design. Once the levee has been built, the dune is constructed from a template to form the initial profile. This initial profile is then scanned.

2. **Calibrate Wave Gauges** - Calibration of the wave gauges involves taking multiple measurements from one wave gauge that is mounted so that its vertical position may be adjusted. The tank is filled to 112 cm and the calibration gauge takes six measurements at 1 cm vertical increments, creating a calibration curve for the single gauge. The calibration gauge is then locked in its test position and the tank is slowly drained. Each subsequent 1 cm drop in water height recorded by the calibrated gauge triggers the others to take a measurement. After six water levels have been measured, the program automatically stops measuring and calculates calibration curves for each of the eight gauges.

3. **Stillwater** - The tank is drained to the design level (102.7 cm in the flume) and allowed to settle until all visible wave movement has stopped. Then, free

surface elevation measurements are taken at 10 Hz for 60 s to record the water level before each test.

4. **Wave Burst** - The wave climate generated from the JONSWAP spectrum is run for 300 s. While the waves are being generated, all eight gauges record water surface elevation measurements at a frequency of 20 Hz.

5. **Profile Scans** - After 5 min, 10 min, 20 min, and 40 min of wave bursts, the beach profile is scanned in order to measure beach profile morphology. The spacing between scans varies along the beach profile in order to obtain high resolution measurements in areas of high change, while saving time in areas of low change. Most scans are taken at an interval of 2 cm, however 1 cm intervals are used where dune erosion takes place in order to precisely capture the steep dune face, and 10 cm spacing is used beyond the point where eroded profiles converge to the initial profile.

Wave climate and data collection procedure for each test and the overall experiment are summarized in Table 3.5. The duration and time intervals between scans were determined by observation of calibration test runs before commencing the experiment. The erosion rate of the dune and profile slowed over time, thus allowing for longer intervals between scans after the first 10 min of wave bursts. 40 min was chosen as an end point during calibration test runs because at that time the dune face had retreated past the peak of the original dune and had eroded enough to expose the core to direct wave attack for a significant time period. Had erosion rates been significantly slowed during any of the tests, such that the dune face had not eroded to the point of the original dune peak, tests would have continued until that point was reached to allow for more core exposure. An exception to this was made for the T-Wall Dune because almost no erosion occurred after the dune face had reached the wall. At full scale, the test time corresponds to roughly three hours of storm, as time is scaled at the square root of the model scale factor. [10] This is not sufficient for modeling an entire storm, however it is roughly equivalent to the duration of peak storm conditions of a large storm event. [9]

Table 3.5: Experimental overview for all four test configurations.

Experiment	Wave Test Time (s)	300 s Wave Bursts	Scans
Single LID	2400 s	8	5
Total	9600 s	32	20

4. DATA ANALYSIS

This section describes the data analysis performed for the LID concept experiment. Analyses of both dune morphology and hydrodynamic conditions are presented.

4.1 Dune and Beach Morphology

Beach and dune morphological changes were analyzed for each LID concept throughout the eight wave bursts. "Profile scans" were taken five times for each test: initially before any waves bursts, after one wave burst (5 min), after two wave bursts (10 min), after four wave bursts (20 min) and after the final wave burst (40 min). The laser profiler takes longshore "slice scans" at numerous cross-shore locations, at intervals between one and ten cm. The ends of each slice scan contained data points along the vertical walls of the flume. A buffer of forty data points was removed to eliminate these edge points. The remaining points were then checked for bad data, which were removed based on intensity level recorded by the scanner. Almost all scans had over two hundred points remaining after the removal of the buffer zones and outliers. Finally, each slice scan was averaged to find a representative elevation for that cross-shore position.

The averaged cross-shore elevations were then combined to form a representative 2-D profile for each of the five profile scans that were taken. 3-D profiles were also made using the entire set of points from each slice scan (after buffer and outlier removal), and used to check for longshore uniformity, one of the underlying assumptions of running the experiment in a narrow wave flume. Only the 2-D profiles were used for quantitative analysis. Figure 4.1 shows the full initial profile scan of the No-Core LID in 3-D, while Figures 4.2 to 4.5 show 3-D profiles (zoomed in to better show regions of active transport) over the entire test for each LID.

Quantifying profile evolution over time produces a good description of the relevant performance differences between each LID concept. This section investigates various aspects of dune and beach morphology - visual profile changes, dune face retreat, submerged beach profile accumulation and cross-sore sediment transport - to better understand the influence of each LID.

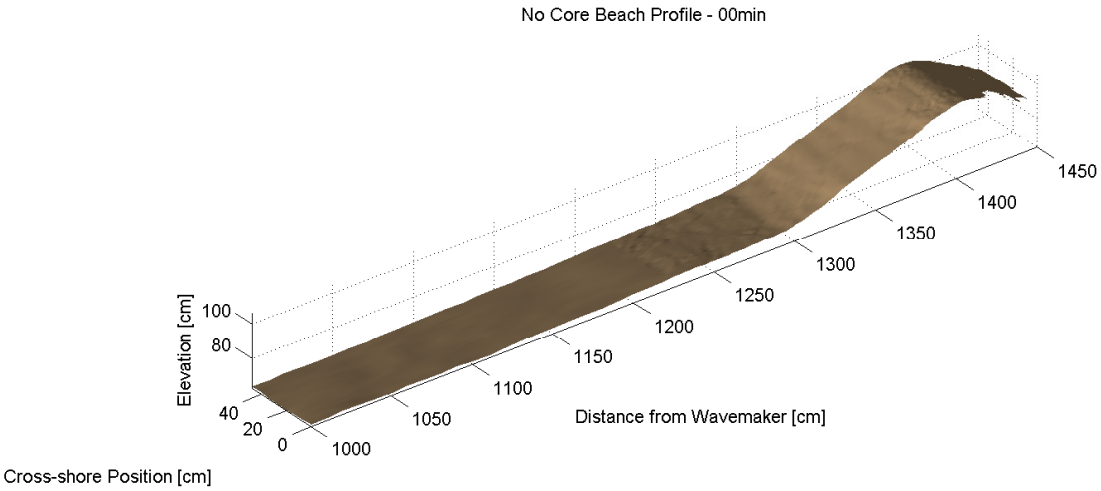

Figure 4.1: Initial No-Core LID profile scan in 3-D showing the entire scanned dune and beach.

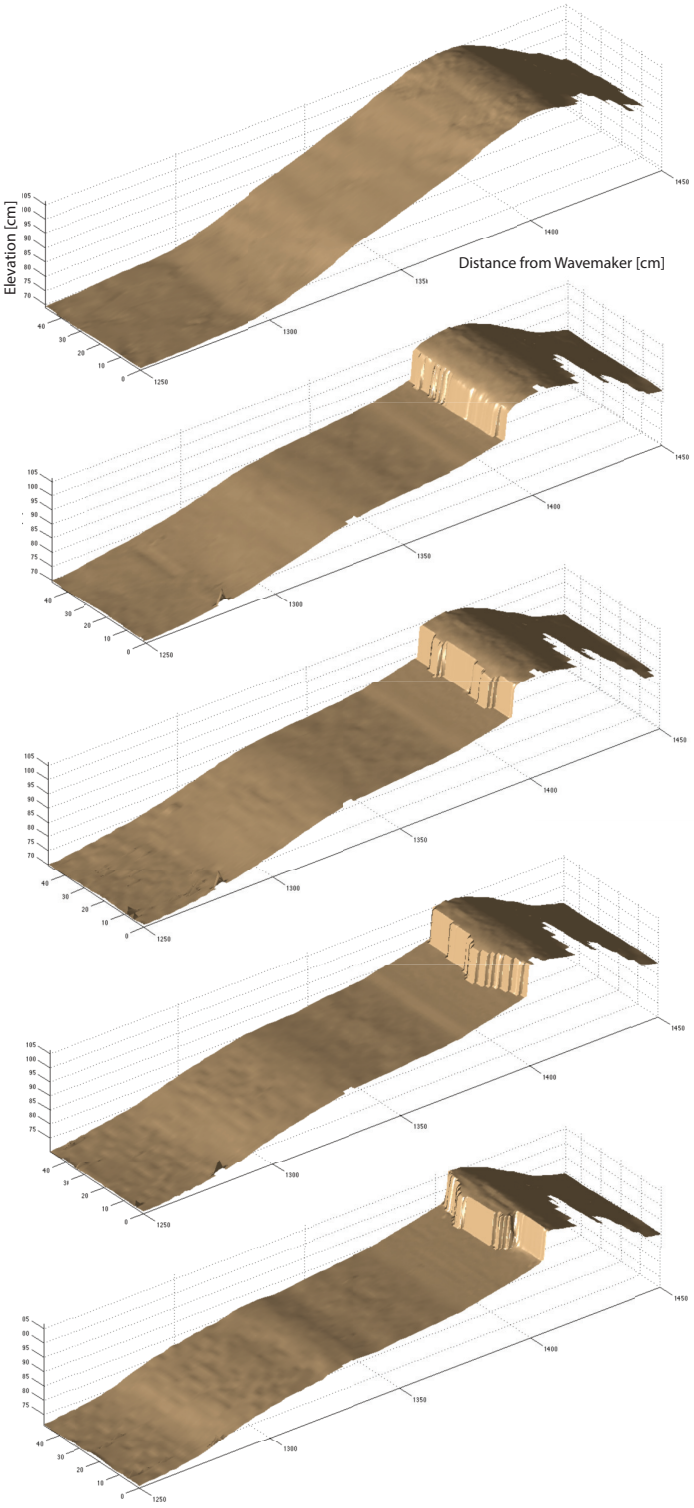

Figure 4.2: Profile change for the No-Core LID in 3-D.

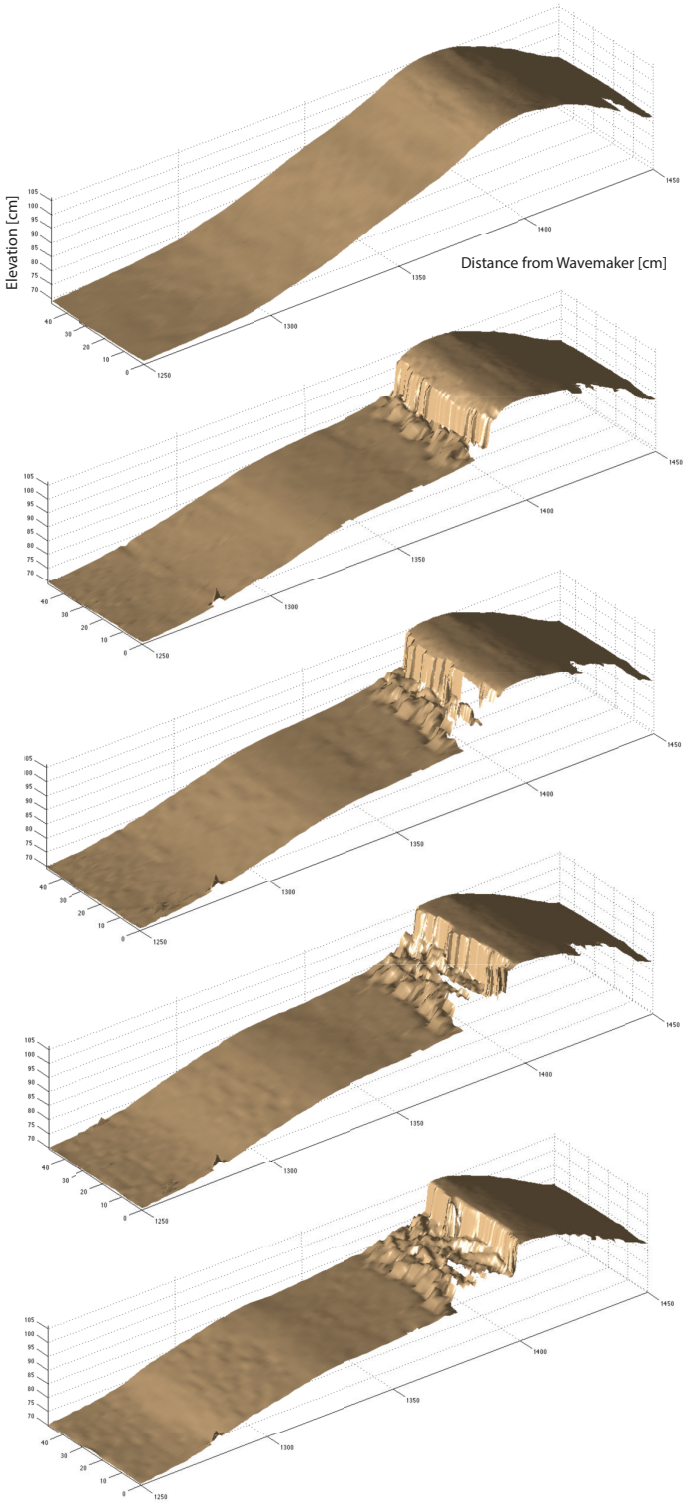

Figure 4.3: Profile change for the Armorstone-Core LID in 3-D.

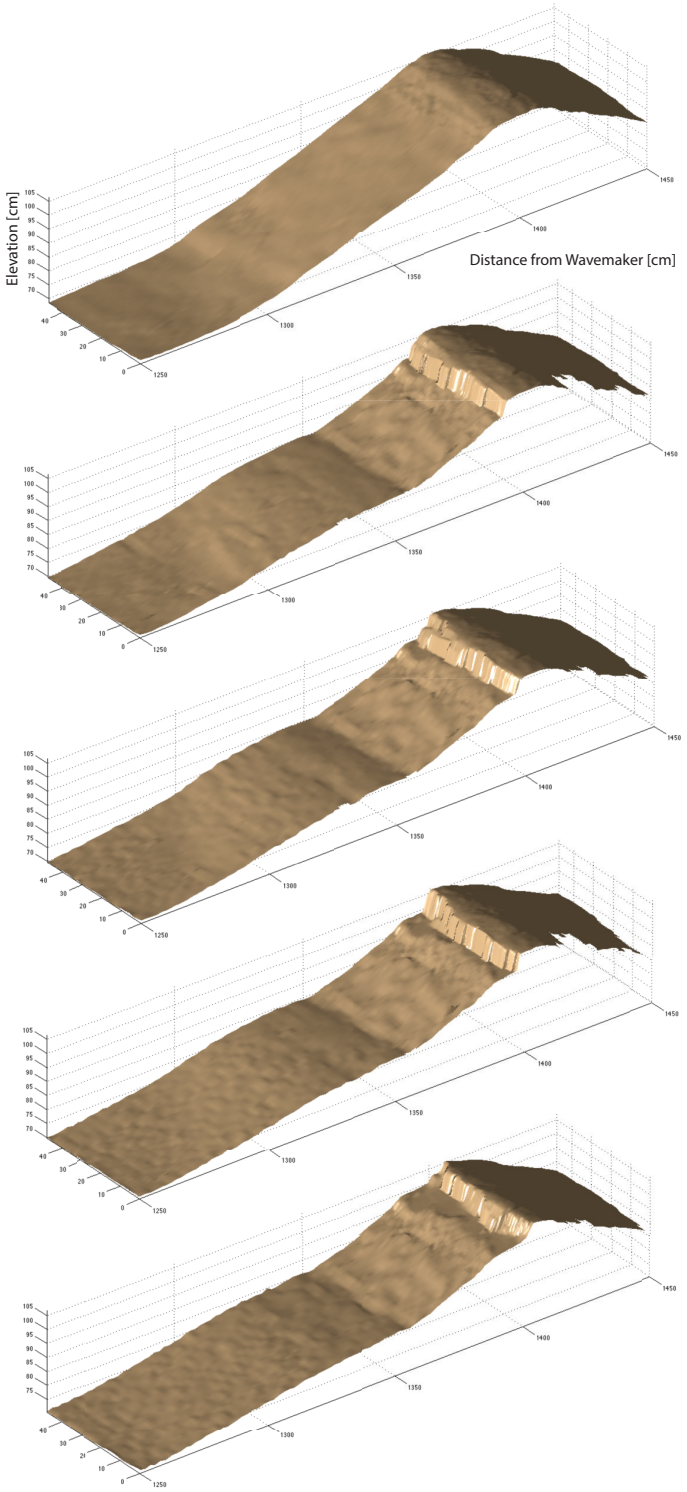

Figure 4.4: Profile change for the Clay-Core LID in 3-D.

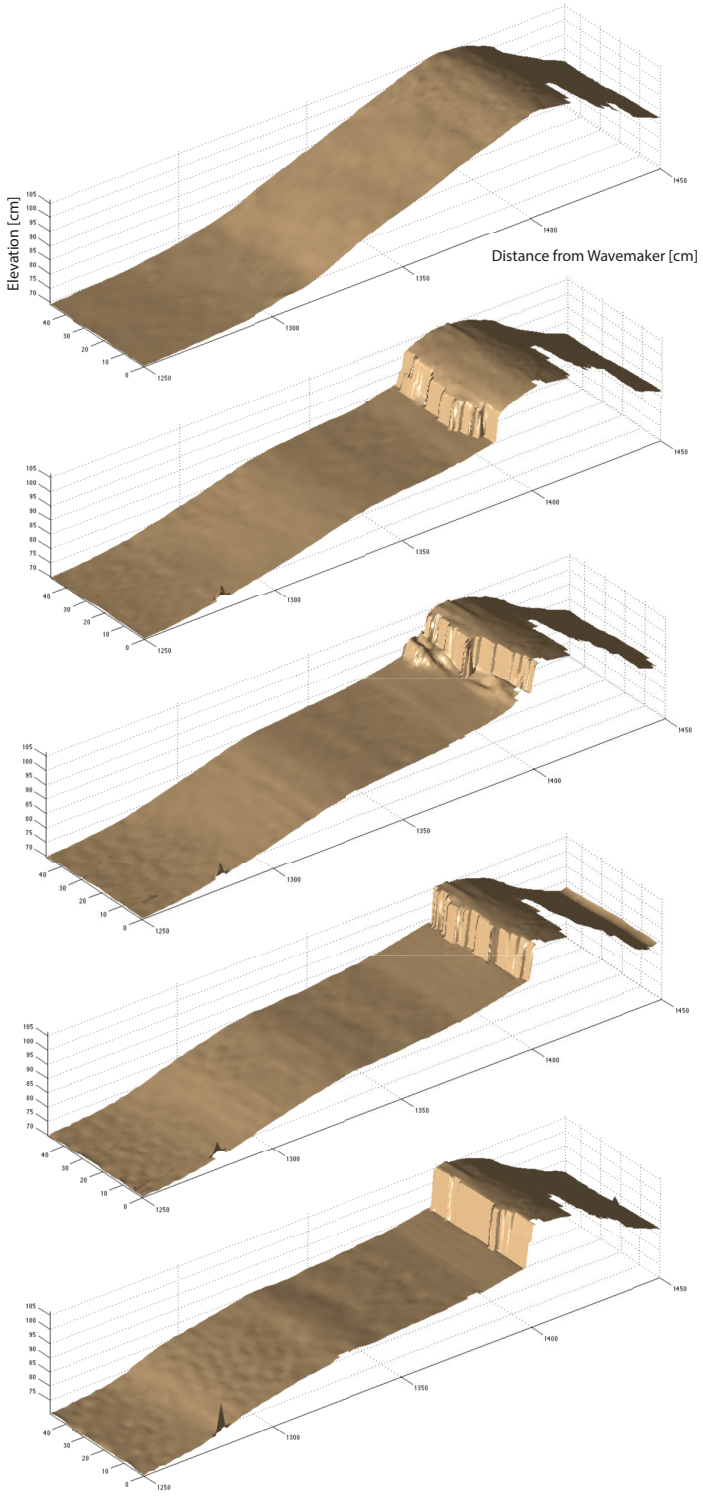

Figure 4.5: Profile change for the T-Wall LID in 3-D.

4.1.1 Profile Evolution

Noting the change in beach profile over the course of the simulated storm test allows for a qualitative analysis and description of beach and dune morphology for each LID concept. Looking at the profile changes and comparing them between LID concepts gives insight into how the dune-structure interaction affects morphology in a more descriptive manner than simply comparing quantitative volume changes.

The four concepts followed a characteristic profile evolution over the course of the test. Initially, the dunes experienced rapid scarping erosion on the front slope, which created a nearly vertical dune face. The heavy erosion caused the dune face to quickly retreat, which was measured as ΔDF_x. The eroded sediment from the dune was deposited offshore, raising the height of the submerged beach profile in the surf zone. Initially, waves were observed breaking just before the dune, and crashing directly into the dune face. The raised submerged profile caused the larger waves to break further offshore, dissipating much of the wave energy in the surf zone rather than directly on the dune face. This phenomenon was amplified as the submerged profile grew in size, and the dune face continued to retreat. Over time the raised submerged profile settled into an equilibrium profile, and its development was measured by finding its center S_x, height above initial profile at center S_h, and water depth at its center S_d. The growing submerged beach profile reduced the direct wave energy hitting the dune face, drastically slowing its rate of erosion and retreat. After all eight wave bursts, the dune face had reached a cross-shore location roughly at the mid point of the initial dune in all cases. However, each LID concept showed distinctive differences in profile change over the course of the test, marking how the core structure affects erosion.

With no structure to protect the dune against shoreline change, the No-Core LID followed the above profile change description. The effect of the submerged beach profile can be seen in Figure 4.6, as it grows, the rate of dune face retreat slows. Considering that each subsequent profile scan was taken at a larger time interval than before, this slowing effect becomes especially apparent. Figure 4.6 shows profile change throughout the No-Core LID test, and Table 4.1 lists values for dune face retreat and submerged beach profile morphology.

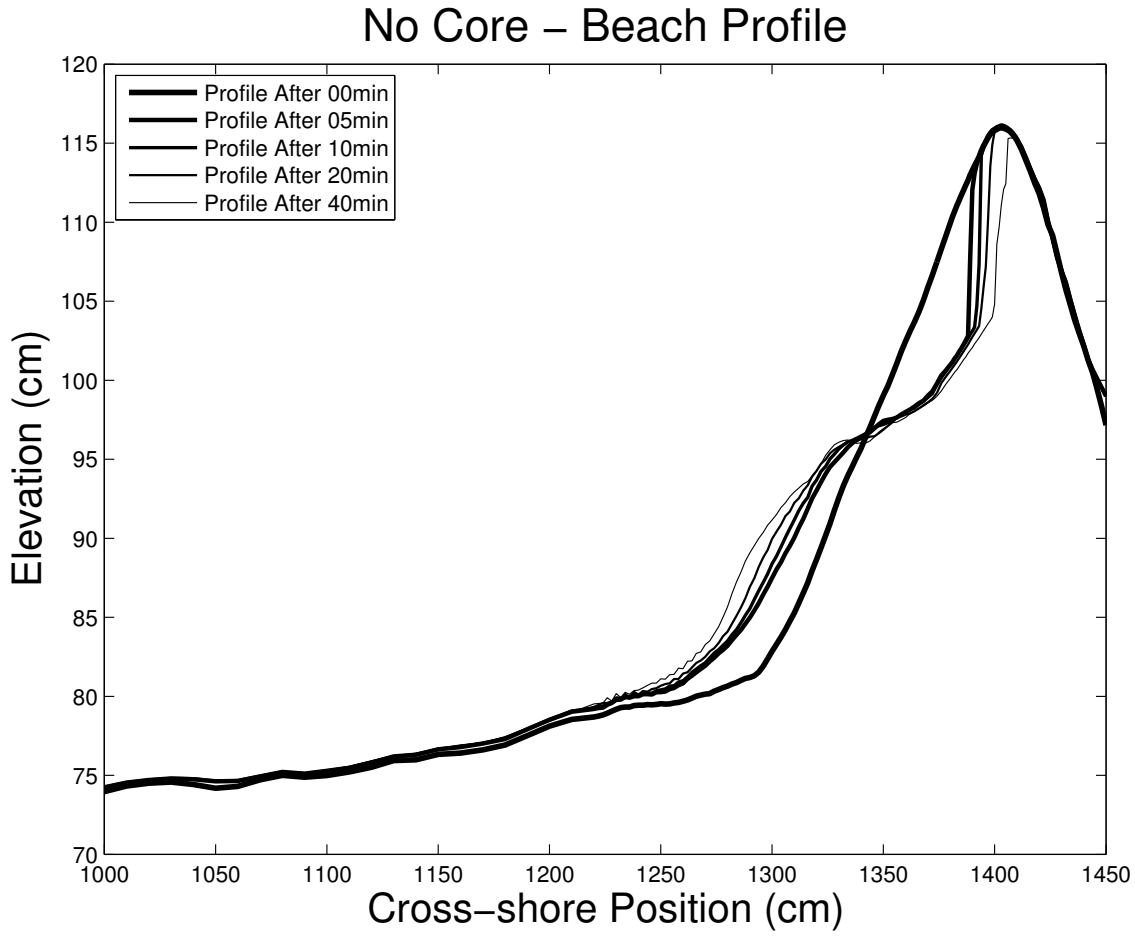

Figure 4.6: Profile change for the No-Core LID.

Table 4.1: Dune face and submerged beach profile morphology for the No-Core LID. Initial dune face location is absolute, while the subsequent values represent change from initial position.

Profile Scan	ΔDF_x [cm]	S_x [cm]	S_h [cm]	S_d [cm]
Initial	1380.2	-	-	-
5 min	9.4	1306	4.8	13.7
10 min	3.8	1310	5.9	11.5
20 min	3.6	1306	7.2	11.3
40 min	5.2	1298	8.5	11.9

The Armorstone-Core LID showed the least variance from the No-Core LID. After two wave bursts (10 min) the erosion began to expose the armorstone revetment. While the core protected the underlying sediment against erosion and the stones did not become dislodged, wave runup was significant enough for erosion and dune face retreat to continue above the core in the sand cover layer. The final profile for the Armorstone-Core LID looked much like the No-Core LID, however the exposed armorstone core remained in place where the No-Core LID had eroded away. Figure 4.7 shows profile change throughout the Armorstone-Core LID test, and Table 4.2 lists values for dune face retreat and submerged beach profile morphology.

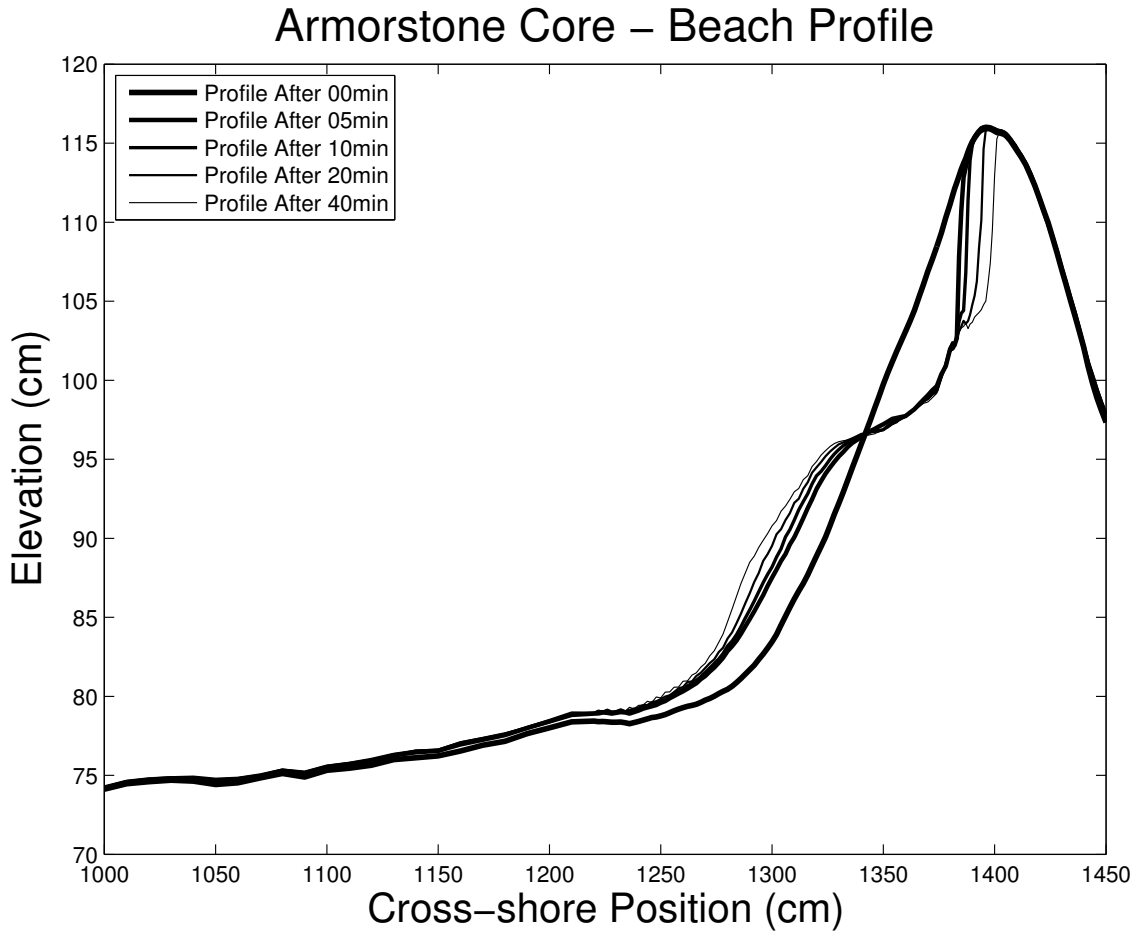

Figure 4.7: Profile change for the Armorstone-Core LID.

Table 4.2: Dune face and submerged beach profile morphology for the Armorstone-Core LID. Initial dune face location is absolute, while the subsequent values represent change from initial position.

Profile Scan	ΔDF_x [cm]	S_x [cm]	S_h [cm]	S_d [cm]
Initial	1374.4	-	-	-
5 min	7.3	1320	4.2	9.6
10 min	3.0	1314	5.2	10.4
20 min	6.2	1302	6.3	12.5
40 min	5.2	1300	7.3	11.9

In contrast, the Clay-Core and T-Wall LID's had significant differences in profile change in comparison to the No-Core LID. After only one wave burst (5 min), the entire sand layer covering the front face of the Clay-Core LID eroded away leaving the flood-slope of the clay levee completely exposed. By this time, the dune face had also retreated farther than any profile after one wave burst. After this initial surge in dune face retreat, the erosion rate was greatly reduced. The clay core was strong enough to withstand the duration of the test with no levee erosion. None of the clay was transported offshore and the final profile shows the same levee outline as the 5 min profile. Given this behavior, significantly less sediment was transported to the offshore submerged beach profile and less wave energy was able to be dissipated offshore from the dune. With more wave energy hitting the hard clay levee directly, more energy was reflected back, which is evident in the wave analysis as well. Figure 4.8 shows profile change throughout the Clay-Core LID test, and Table 4.3 lists values for dune face retreat and submerged beach profile morphology.

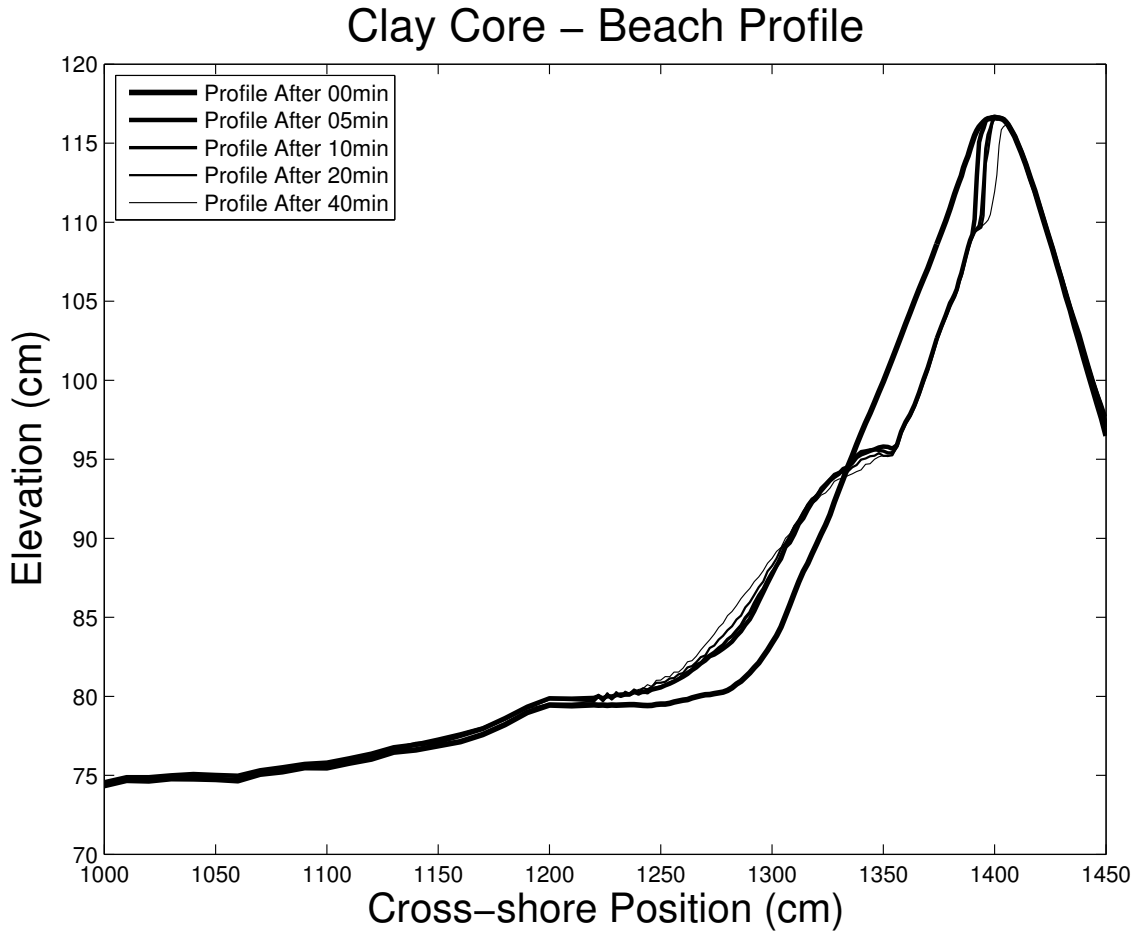

Figure 4.8: Profile change for the Clay-Core LID.

Table 4.3: Dune face and submerged beach profile morphology for the Clay-Core LID. Initial dune face location is absolute, while the subsequent values represent change from initial position.

Profile Scan	ΔDF_x [cm]	S_x [cm]	S_h [cm]	S_d [cm]
Initial	1377.8	-	-	-
5 min	13.0	1302	4.4	14.4
10 min	2.6	1304	4.5	13.8
20 min	1.1	1298	5.0	14.8
40 min	1.7	1298	5.5	14.3

The T-Wall LID had the most drastic effect on profile morphology of all the LID concepts. Initially, the erosion began just as the No-Core dune had, with almost identical profiles after one wave burst (5 min). However, between wave bursts one and two, the dune face experienced very rapid erosion until hitting the vertical face of the T-Wall. The vertical wall completely halted dune face retreat for the remainder of the test, with almost no erosion occurring above the wall. Since the T-Wall blocked any erosion from taking place beyond it, the profile began to erode downward rather than backward as in the other cases. Wave runup hit the T-Wall and bounced back rather than continuing up and pushing the dune face back. As waves continued to hit the wall, the height of the beach profile in front of the wall continued to sink. The final profile consisted of the intact back and top of the dune, a vertical drop at the T-Wall's front face and a shallow beach slope that transitioned very smoothly into the submerged beach profile. Figure 4.9 shows profile change throughout the T-Wall LID test, and Table 4.4 lists values for dune face retreat and submerged beach profile morphology.

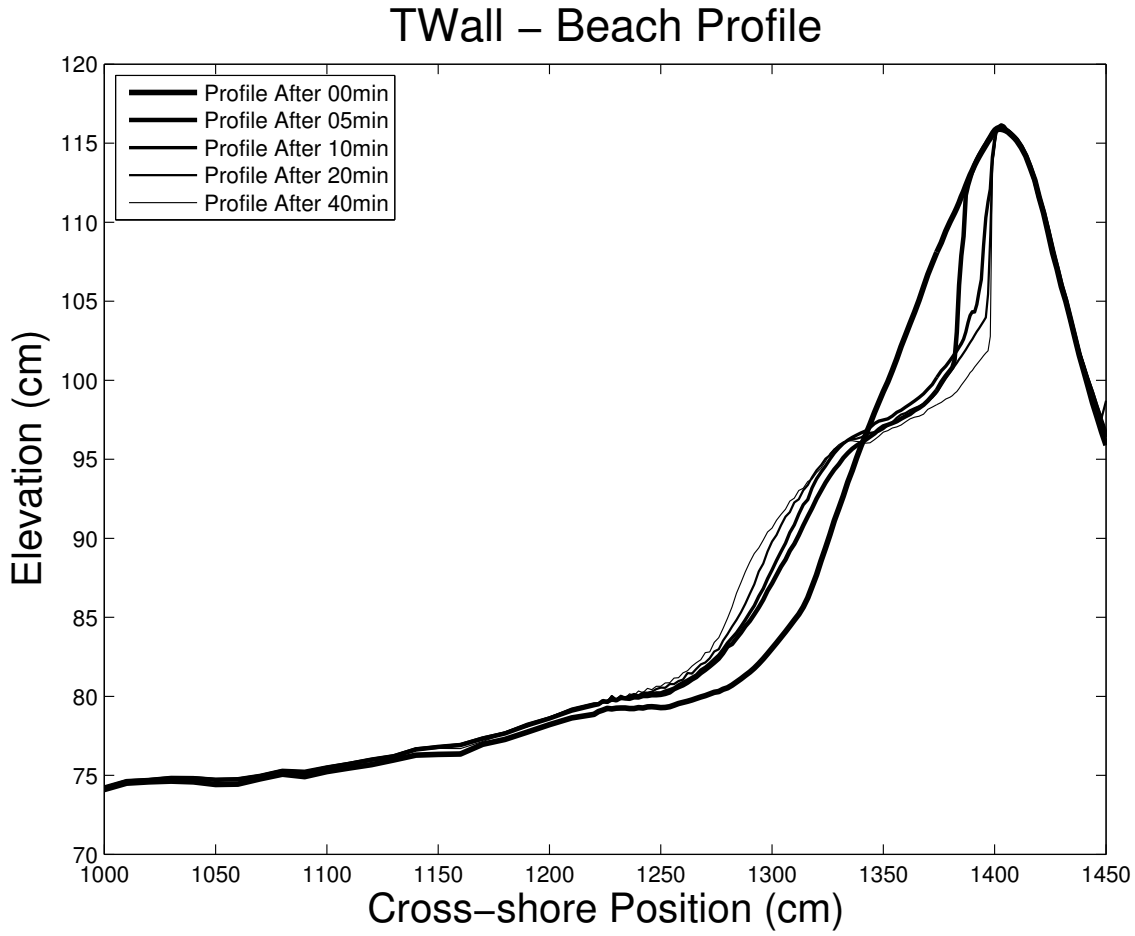

Figure 4.9: Profile change for the T-Wall LID.

Table 4.4: Dune face and submerged beach profile morphology for the T-Wall LID. Initial dune face location is absolute, while the subsequent values represent change from initial position.

Profile Scan	ΔDF_x [cm]	S_x [cm]	S_h [cm]	S_d [cm]
Initial	1379.9	-	-	-
5 min	6.5	1314	5.2	11.9
10 min	9.4	1314	6.5	10.6
20 min	2.4	1310	7.4	10.4
40 min	0.5	1308	7.9	10.3

4.1.2 Erosion and Accretion

Evaluating changes in beach profiles reveals areas of accretion and erosion. The profile changes provide a visual depiction of the underlying cross-shore sediment transport causing the erosion and accretion, however quantitative results are desired as well for a meaningful understanding of the underlying mechanisms. This section describes how numerical values for erosion and accretion where found. Differences between the LID concepts illustrate how the presence of each structure uniquely influences dune and beach morphology.

Active transport regions, the eroding dune face, and accreting submerged offshore beach profile are identified for the focus of this analysis. To identify the exact location of each region, the cross-shore position of each boundary must be determined. The two regions border one another, meaning the transition from erosion region to accretion region can be used as a common boundary location for each region. Figure 4.10 shows an example of typical areas of accretion and erosion for each test.

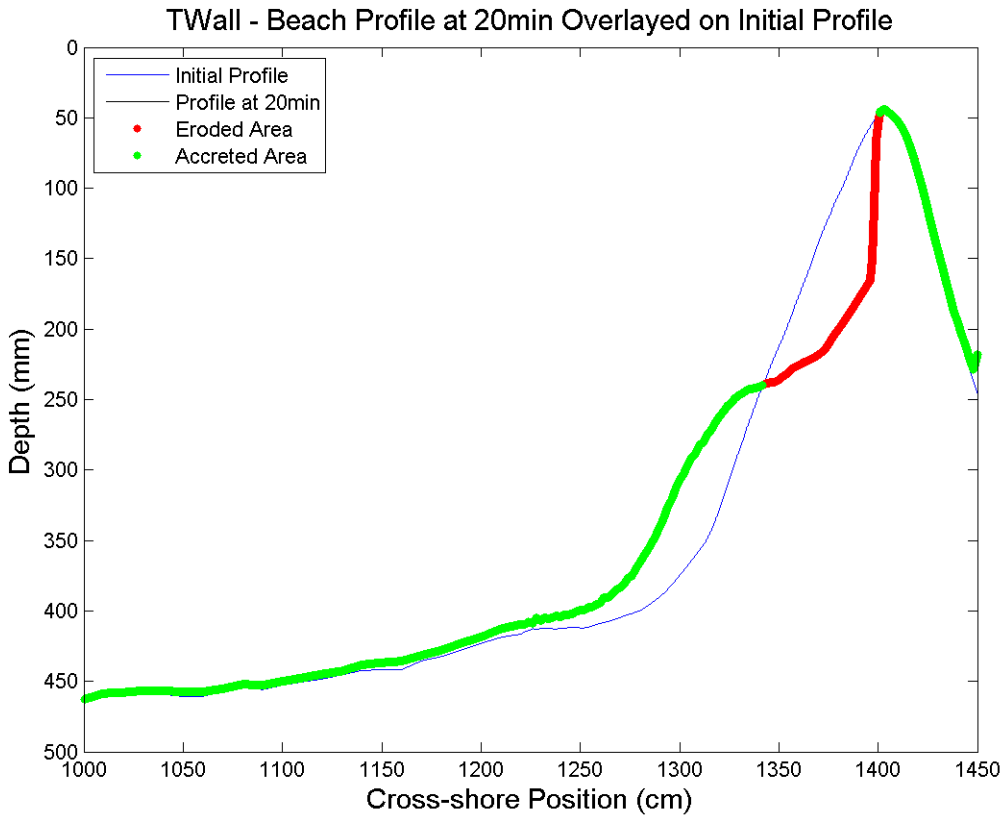

Figure 4.10: T-Wall LID profile showing erosion and accretion regions with initial profile overlaid to show change.

This common boundary changes as dune morphology progresses, so the boundary cannot be fixed, it must change with the morphology of the beach profile. In order to find its location, the averaged beach profile for each profile scan is compared to the initial averaged beach profile and the transition from erosion region to accretion region is calculated for that profile scan. The last profile scan is along the back face of the dune at a cross-shore location of 1450 cm, so this location was chosen as the starting boundary of the dune. The end boundary of the accretion region was chosen by comparing profiles over time and determining where shoreline changes became unnoticeable. The exact location was fine tuned based on performing a sediment volume balance between erosion and accretion regions. Since there is very little sediment lost, the volume gained in the accretion region should match that

lost in the erosion region. By finding the location at which the two volumes become almost equal, the boundary of the accretion region can be determined.

To find the cumulative volume of sediment eroded and accreted, V_e and V_a, the difference between the current and initial beach profiles is integrated using a trapezoidal method in both regions. This is done for each profile scan. To find the change between intermediate profile scans (for example the change between scan two and scan three), the cumulative change from the former profile scan is subtracted from that of the latter. Tables 4.5 to 4.8 summarize the results of the volume change analysis for each LID.

Table 4.5: Profile sand volume changes for the No-Core LID. $\%V_e$ represents the ratio of eroded volume to initial dune volume.

	Cumulative			Individual Wave Burst		
Profile Scan	V_e $[cm^2]$	V_a $[cm^2]$	$\%V_e$	V_e $[cm^2]$	V_a $[cm^2]$	$\%V_e$
Initial	0	0	0%	0	0	0%
5 min	247	281	21%	247	281	21%
10 min	289	328	25%	42	47	4%
20 min	345	389	29%	56	61	4%
40 min	433	467	35%	88	78	6%

Table 4.6: Profile sand volume changes for the Armorstone-Core LID. $\%V_e$ represents the ratio of eroded volume to initial dune volume.

	Cumulative			Individual Wave Burst		
Profile Scan	V_e $[cm^2]$	V_a $[cm^2]$	$\%V_e$	V_e $[cm^2]$	V_a $[cm^2]$	$\%V_e$
Initial	0	0	0%	0	0	0%
5 min	240	256	20%	240	256	20%
10 min	271	302	22%	31	46	2%
20 min	339	358	28%	68	56	6%
40 min	410	419	33%	71	61	5%

Table 4.7: Profile sand volume changes for the Clay-Core LID. $\%V_e$ represents the ratio of eroded volume to initial dune volume.

	Cumulative			Individual Run		
Profile Scan	V_e $[cm^2]$	V_a $[cm^2]$	$\%V_e$	V_e $[cm^2]$	V_a $[cm^2]$	$\%V_e$
Initial	0	0	0%	0	0	0%
5 min	275	244	19%	275	244	19%
10 min	305	259	21%	30	15	2%
20 min	312	286	21%	7	27	0.5%
40 min	352	311	23%	40	25	2%

Table 4.8: Profile sand volume changes for the T-Wall LID. $\%V_e$ represents the ratio of eroded volume to initial dune volume.

	Cumulative			Individual Run		
Profile Scan	V_e $[cm^2]$	V_a $[cm^2]$	$\%V_e$	V_e $[cm^2]$	V_a $[cm^2]$	$\%V_e$
Initial	0	0	0%	0	0	0%
5 min	235	272	20%	235	272	20%
10 min	315	332	28%	80	60	8%
20 min	373	395	32%	58	63	4%
40 min	447	448	37%	74	53	5%

The quantitative volume changes reflect the visual analysis of each LID's profile change throughout its test. The No-Core and Armorstone-Core LID's had almost identical eroded volumes at each profile scan, with the bulk to the erosion happening in the first wave burst. The Clay-Core LID experienced the most erosion in the first wave burst and then saw very little erosion for the remainder of the test. For the first wave burst, the T-Wall LID's erosion was very similar to the No-Core and Armorstone-Core LID's, however the erosion for the second half of the test was the highest seen of all the LID concepts.

4.2 Hydrodynamics

Recording and analyzing wave data is necessary in order to fully understand the conditions present during testing. While the analysis does not give any direct knowledge of dune morphology, some insight can by gained by looking at how certain wave parameters change with each configuration and over time. From this, the forcing conditions responsible for specific morphology changes can be interpreted. During wave bursts, free surface elevation was measured at eight locations along the wave flume. Three gauges were placed in deep water, three in the surf and swash zones and the remaining two spread across the transition region. Data were collected during the entire wave burst, however data for the first 20 s of each time series were removed before analysis to allow for sufficient wave climate development to occur.

Tables 4.9 to 4.12 present deep-water wave climate statistics recorded by WG3 for each of the four LID concepts, which include both incident and reflected waves. The tables present significant wave height (H_s), normalized significant wave height ($H_s/H_{s,initial}$), mean wave height (H_{mean}), significant period (T_s), and the number of waves used to generate the statistics. Individual waves are found using a zero up-crossing method and the associated wave height and period are recorded for each wave. The mean wave height is calculated as simply the average value of those heights. Significant wave height is defined as the average of the one-third highest wave heights. In order to calculate H_s, the wave heights are first sorted and then averaged taken of the greatest one-third of the values. Significant period is simply the average period of the waves with the one-third highest wave heights. Since initial significant wave height varies slightly in the Clay-Core test, normalized significant wave height is presented to provide a direct comparison.

The general trend among the tests is that H_s decreases over time, with the exception of the Clay-Core LID. As the dune face erodes and forms a more gradual slope and submerged offshore beach profile, more wave energy is absorbed by the beach and less is reflected back. The Clay-Core LID did not erode nearly as much as the other concepts, and the solid clay levee acted as an efficient reflector. Not only did wave heights not decrease as much over time, the Clay-Core LID tests recorded significantly more wave energy than the others. The smallest H_s recorded in the Clay-Core LID tests is larger than any H_s recorded in any of the other three concept tests.

Table 4.9: Deep water wave statistics for the No-Core LID experiment. All values are taken from WG 3.

Run	H_s [cm]	$H_s/H_{s,initial}$ [cm]	H_{mean} [cm]	T_s [s]	Number of Waves
5 min	7.7	1.0	5.0	1.06	263
10 min	7.2	0.94	4.7	1.06	259
15 min	7.1	0.92	4.7	1.07	260
20 min	7.1	0.92	4.7	1.08	257
25 min	7.2	0.94	4.7	1.05	261
30 min	7.2	0.94	4.7	1.08	259
35 min	7.2	0.94	4.7	1.06	264
40 min	7.2	0.94	4.7	1.05	264

Table 4.10: Deep water wave statistics for the Armorstone-Core LID experiment. All values are taken from WG3.

Run	H_s [cm]	$H_s/H_{s,initial}$ [cm]	H_{mean} [cm]	T_s [s]	Number of Waves
5 min	7.7	1.0	4.9	1.10	255
10 min	6.9	0.90	4.3	1.07	260
15 min	6.8	0.88	4.4	1.03	263
20 min	6.9	0.90	4.4	1.03	261
25 min	6.9	0.90	4.4	1.04	263
30 min	6.9	0.90	4.4	1.06	260
35 min	6.9	0.90	4.4	1.07	259
40 min	6.9	0.90	4.4	1.07	260

Table 4.11: Deep water wave statistics for the Clay-Core LID experiment. All values are taken from WG3.

Run	H_s [cm]	$H_s/H_{s,initial}$ [cm]	H_{mean} [cm]	T_s [s]	Number of Waves
5 min	8.4	1.0	5.3	1.03	258
10 min	8.2	0.98	5.1	1.05	265
15 min	8.0	0.95	5.0	1.01	266
20 min	8.0	0.95	5.0	1.00	268
25 min	8.1	0.96	5.1	1.02	264
30 min	8.0	0.95	5.0	1.02	269
35 min	8.1	0.96	5.0	1.00	268
40 min	8.1	0.96	5.1	1.00	267

Table 4.12: Deep water wave statistics for the T-Wall LID experiment. All values are taken from WG3.

Run	H_s [cm]	$H_s/H_{s,initial}$ [cm]	H_{mean} [cm]	T_s [s]	Number of Waves
5 min	7.7	1.0	4.9	1.11	257
10 min	7.1	0.92	4.5	1.07	258
15 min	7.1	0.92	4.6	1.09	254
20 min	7.1	0.92	4.7	1.08	259
25 min	7.1	0.92	4.6	1.04	262
30 min	7.1	0.92	4.6	1.04	266
35 min	7.1	0.92	4.6	1.05	263
40 min	7.1	0.92	4.6	1.05	264

4.3 Discussion of Results

4.3.1 Morphology

All LID concepts experienced similarities in profile morphology over the course of the experiment, yet each displayed unique characteristics as well. Here, the data are

analyzed in a series of figures in a more comparative manner in order to better see differences between LID performance. Additional figures can be found in Appendix C.

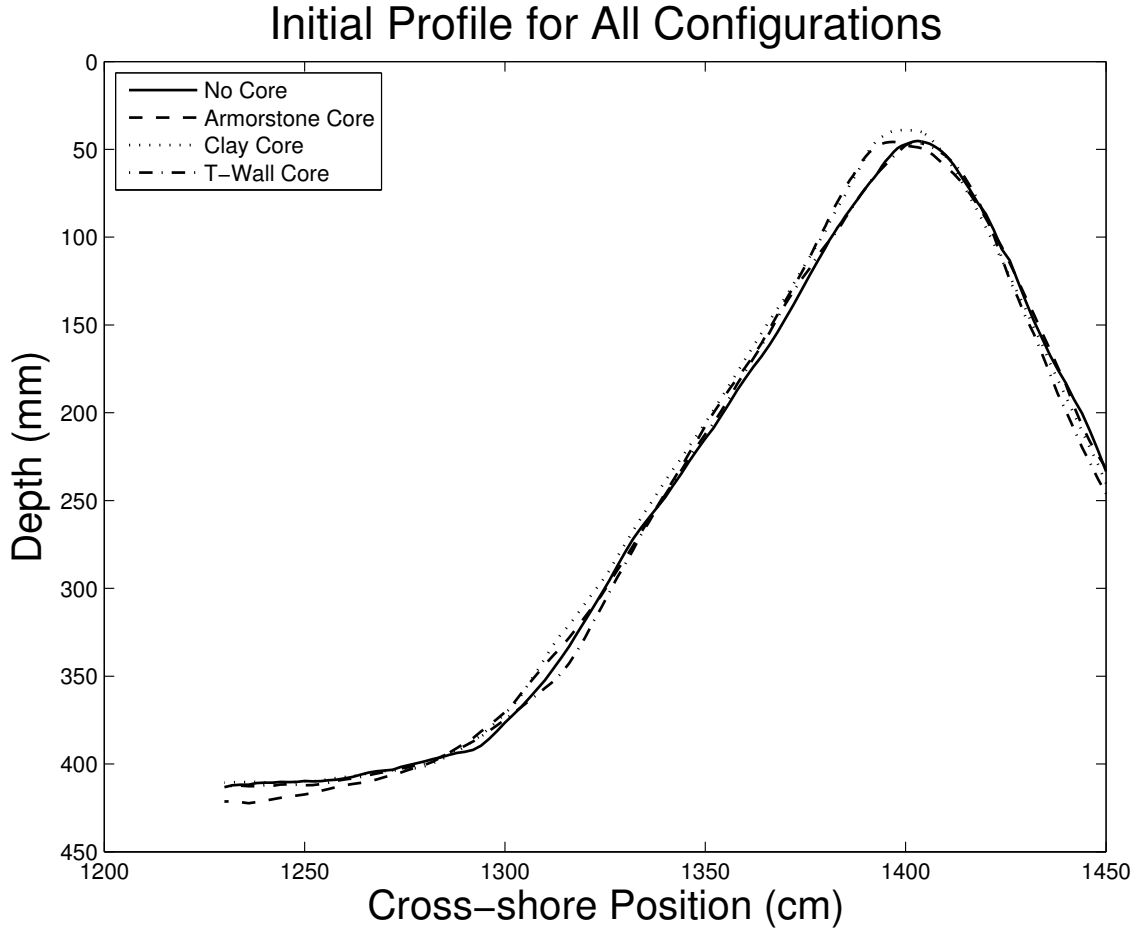

Figure 4.11: Initial profile scans for each LID.

Figure 4.11 shows initial profile scans for each LID. Minimal differences in initial profiles are present, however not considered significant enough to dramatically alter the test results. However, Figure 4.12, showing the final profiles, highlights the differences in dune morphology. The Armorostone-Core LID seems to have subsided slightly as the armorstone layer (visible) was initially built at the same height as the

clay levee. The least change occurs by the Clay-Core LID, as the core stayed fully in tact. The T-Wall's low profile is evident as the profile began to scour down rather than being able to erode back once the dune face hit the T-Wall structure.

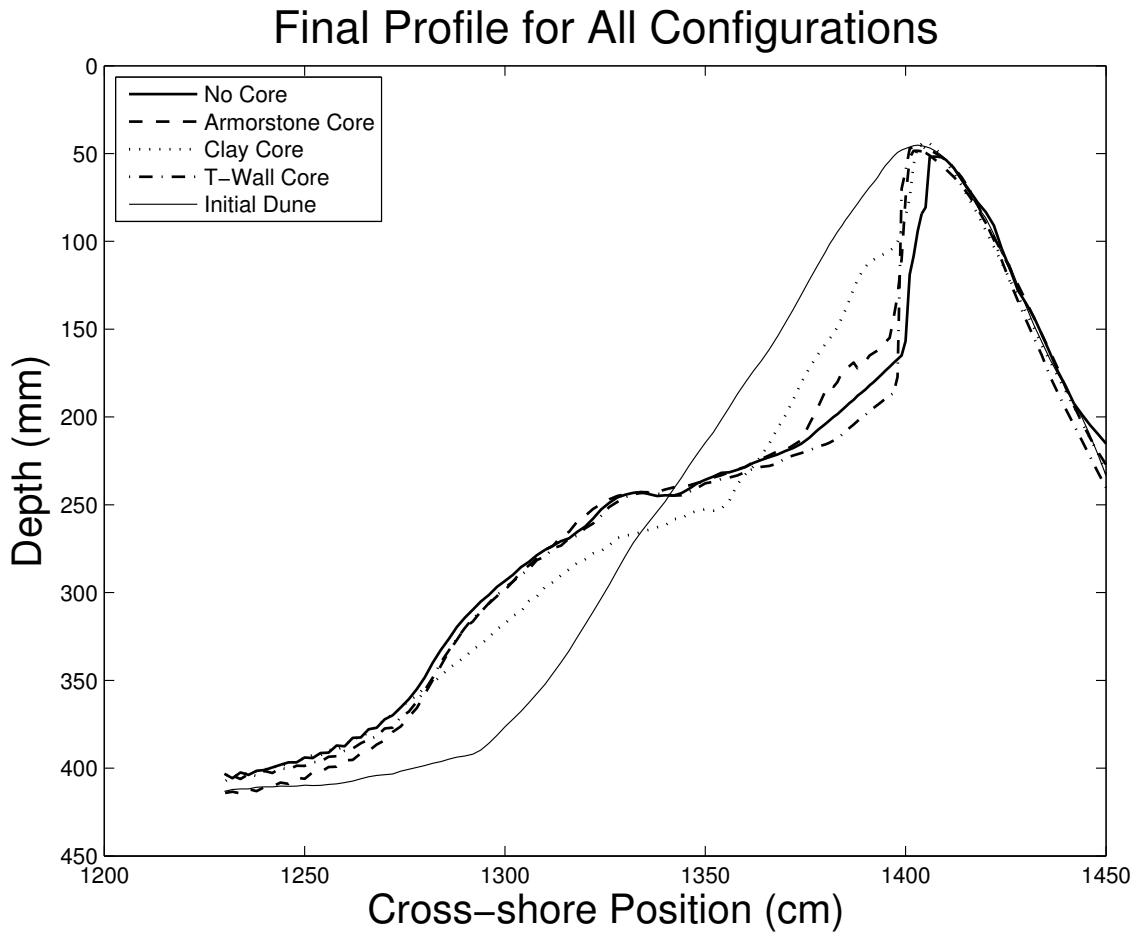

Figure 4.12: Final profiles highlight the differences in dune morphology. Here the initial profile for the No-Core LID is overlayed to emphasize profile change.

Figure 4.13 shows the submerged offshore beach profile formation for each LID concept. The T-Wall LID seems to have produced the largest accumulation in the submerged profile, suggesting an increase in dune erosion. The Clay-Core LID, generating noticeably the smallest submerged profile, is again clearly and substantially

different from the other concepts. Figure 4.14 shows the dune face retreat for each LID concept. It can be seen that the Clay-Core LID and T-Wall LID experienced rapid initial retreat which substantially declined after early wave bursts, while the No-Core LID and Armorstone-LID experienced more gradual decline in dune face retreat rate.

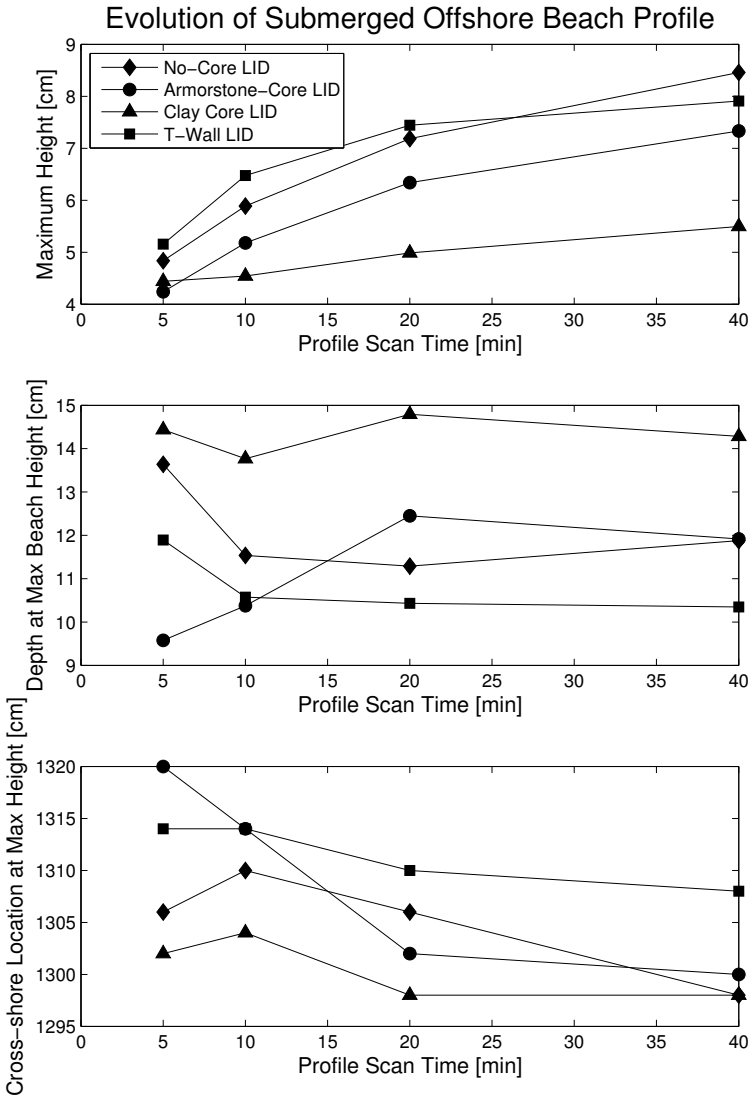

Figure 4.13: Submerged offshore beach profile formation for each LID concept.

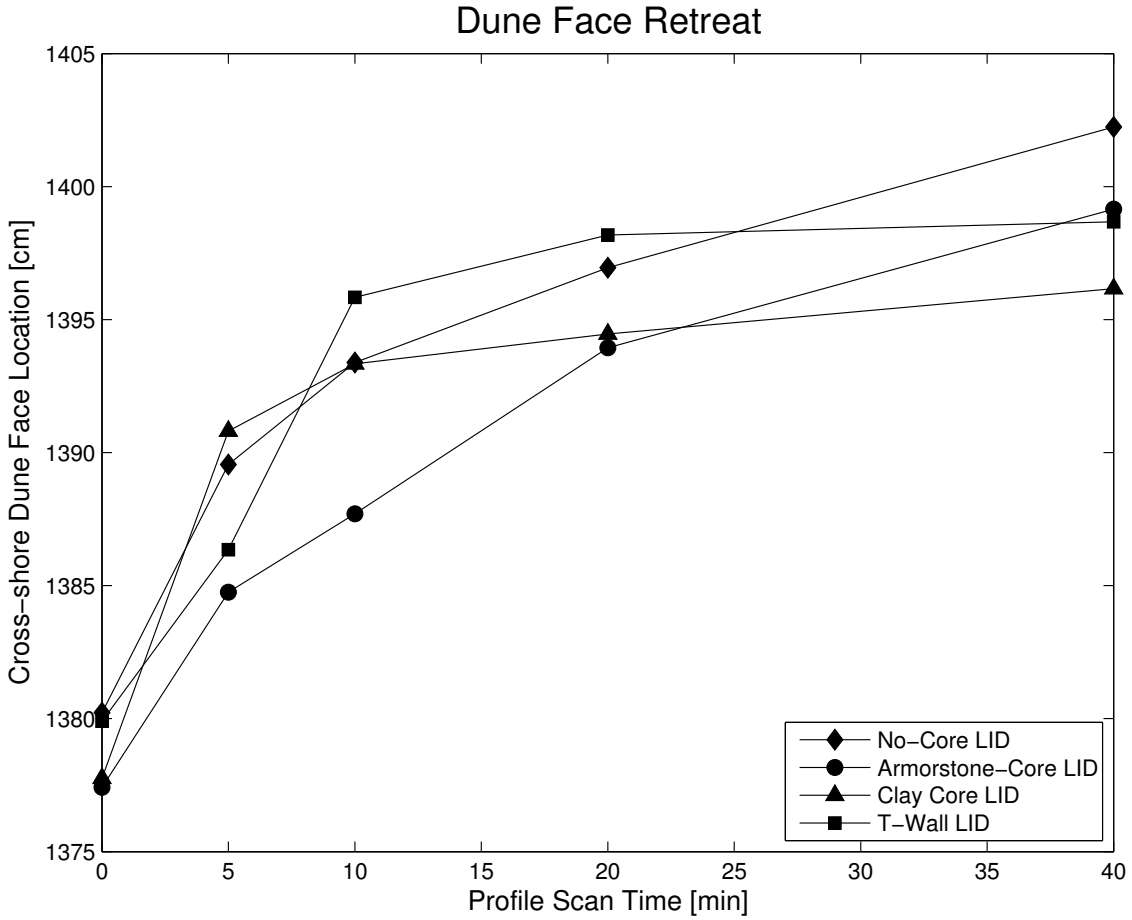

Figure 4.14: Dune face retreat for each LID concept.

Cumulative erosion for all LID's are expressed in Figure 4.15 as a percentage of initial dune volume. Consistent with profile change analysis, the T-Wall LID underwent the most erosion, while the Clay-Core LID experienced the least. No-Core and Armorstone-Core LID's experienced very similar erosion.

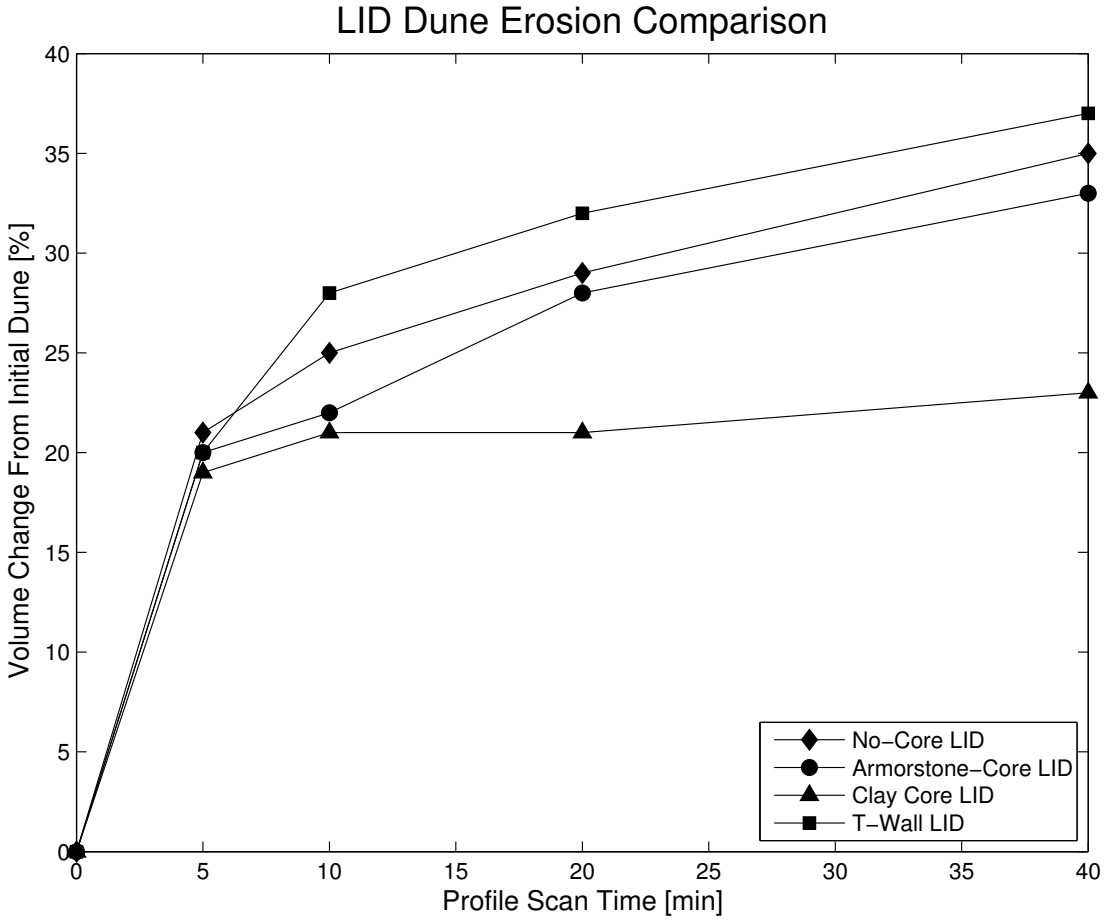

Figure 4.15: Cumulative erosion for all LID's expressed as a percentage of initial dune volume.

4.3.2 Wave Climate

Analyzing the wave climate produced statistics that showed that as beach profiles eroded and began to form shallower slopes and an accumulation in offshore beach profile, the amount of total wave energy decreased. This is because the changes in dune morphology increased the beach's effectiveness at wave energy absorption. Less wave energy was reflected back offshore and subsequently recorded by the deep water wave gauge. Wave statistics calculated for the Clay-Core LID indicate that the clay levee acts to reflect wave energy more than a sandy beach.

5. CONCLUSIONS

5.1 Design Considerations

The initial design concepts for the Ike Dike fixed barrier include four Levee-in-Dune alternatives. Traditional coastal levees were covered with a layer of sand to give the appearance of a natural sand dune while forming a protective barrier against hurricane surge and wave attack. The design alternatives utilize four distinct cores: sand levee (no-core), armorstone revetment, clay levee, and concrete T-Wall with added reinforcement for stability and seepage control. A summary of the design study is presented in Table 5.1. However, further design refinement is necessary. Many aspects of these designs will need to be further considered and possibly changed.

Table 5.1: Important design parameters, calculated material requirements and estimated cost for each LID concept.

Concept	No Core	Armorstone	Clay	T-Wall
Height [m]	5.2	5.2	5.2	5.2
Sand Layer Thickness [m]	1.0	1.0	1.0	1.0
Crest Width [m]	3.0	3.0	3.0	3.0
Total Footprint Width [m]	53.0	53.0	40.5	40.5
Flood-Side Slope [-]	1v:3h	1v:3h	1v:3h	1v:3h
Land-Side Slope [-]	1v:5h	1v:5h	1v:3h	1v:3h
Sand Volume [m^3/m]	174.3	158.9	39.2	130.8
Core Volume [m^3/m]	-	15.3	96.3	4.7
Total Volume [yd^3/yd]	174.3	174.3	135.5	135.5
Cost [$\$M/mi$]	5.7-6.1	6.1-11.5	3.4-5.7	33.6

The No-Core LID is the most simple design presented in this thesis. The design requires only sand, which can be dredged from offshore or taken from local quarries. This also means that the No-Core LID would be the simplest to construct, and reduces cost. However, the simple design comes at a cost. As the name implies, the

No-Core LID has no protective core, meaning that its only defense against storm surge is reliant solely upon the amount of material in the dune. This, combined with the threat of seepage through the high porosity sand requires the design to have a much larger footprint than concepts with less permeable cores. Reinforcing the dune with an armorstone layer (the Armorstone-Core concept) can protect the dune from scarping, however will not prevent seepage through the dune. This means that even though the dune is reinforced, its width cannot be reduced.

The Clay-Core LID offers the reinforcement similar to the Armorstone-Core LID, with the added benefit of preventing seepage, since clay has such low permeability. This allows the LID to be significantly narrower than an LID with a sand core. However since a Clay-Core LID is still considered a "soft" structure, it still runs the risk of erosion, and subsequently failing. Initial testing for this thesis shows that clay is resilient against scarping erosion, however scale effects make this result questionable. At small-scale the ratio of cohesive forces to wave forces is quite high. At full scale, however, the cohesive strength of the clay remains the same while the wave forces increase significantly.

The T-Wall LID has substantial design flexibility over the other LID concepts. Since the T-Wall itself has a very small footprint, it is possible to greatly reduce the width of the dune itself, which would in turn reduce costs and space requirements. With the addition of stairs, ramps, or walkways, the dune would not need to follow the 1v:3h slope requirement which restricts the width of the footprint for the other concepts. In this case the sand could be piled much steeper, which could reduce the footprint by up to 40 %.

In both New Orleans and the example design, the T-Walls stand alone and must provide complete support for the hydraulic head caused by the storm surge. As a result, the wall must be thick and the base wide in order to withstand and counteract the moment caused by the hydraulic head of the surge which acts to topple the structure. Covered by a sand dune, the Ike Dike T-Walls would be able to be reduced in both thickness and footprint. Even if the dune has completely eroded away ahead of the wall, the sand behind the wall creates a back pressure that would counteract the moment created by the storm surge, allowing for a design with reduced thickness, width and pile length. The material reduction along with the increased ease of construction with the smaller dimensions will noticeably reduce the cost of construction as well.

Cost estimates presented in this thesis were based on studies collecting data from projects around the world. The cost of projects are highly dependent on local factors such as availability of materials and resources, and may be inaccurate for the GHMA. Substantial effort would be required to obtain accurate cost estimates before a design concept is finalized.

The final design for the Ike Dike's fixed barrier will likely be composed of a hybrid design with multiple types of LID's at different locations. Due to many considerations such as available land, level of development and ease of access, what works best for one location may not be best for the entire 84 km span. The possibility of combining designs, such as an LID comprised of a clay levee reinforced by a T-Wall, which could possibly creating a design just as robust as the T-Wall LID with significantly less erosion.

5.2 Physical Modeling

During physical model testing, several interesting findings were made. Morphology changes showed common behavior among the four design, most notably, the development of the submerged offshore beach profile. As sediment eroded from the dune and was deposited offshore, the submerged profile grew, which reduced the intensity of the wave attack directly hitting the LID. This self-protecting mechanism drastically affected how wave energy was dissipated an undoubtedly altered dune morphology.

Over the course of the experiment, the LID concepts lost between 23% and 37% of their total volume to erosion. The No-Core and Armorstone-Core LID's showed very similar trends in both profile change and quantitative erosion analysis. After a period of rapid dune face erosion and subsequent accumulation of the offshore submerged beach profile, the wave energy was dissipated over a larger region and the dune erosion slowed significantly. In this test, the Armorstone-LID did not show a significant advantage over the No-Core LID.

The Clay-Core LID saw the least erosion as the levee core withstood the wave attack. Once the sand layer had been eroded away, the clay levee withstood the wave forces without deteriorating. However, the Clay-Core LID also saw the largest initial erosion rates. The smooth interface between clay and sand may have allowed the sand layer to "slip" of the clay core much faster than it would with other core materials. After losing the entire sand layer in the first wave run, very little material

eroded in subsequent wave runs. However, at full-scale, the clay may not be strong enough to withstand the full force of hurricane conditions, and testing at a larger scale is needed.

The T-Wall LID saw the most overall erosion and developed the largest offshore submerged beach profile of the four concepts. Although dune face retreat was completely stopped at the T-Wall, the presence of the wall may have reflected wave energy back towards the sand just before the wall, causing erosion to happen more quickly in front of the wall. Once the dune face reached the wall, a scouring effect was observed as the energy that would normally be dissipated running up the dune was directed down to the sand at the base of the wall. The scouring caused more sand to be eroded from the dune than in other LID concepts.

Wave statistics were calculated for a deep water location. Trends showed that the evolving beach profile became more efficient at absorbing wave energy as it became more shallow and the submerged berm grew. The Clay-Core LID recorded more wave energy than any other concept, caused by its low erosion and steeper slope.

The testing shows that different LID cores can have noticeable effects on profile morphology.

5.3 LID Concept Comparison

Overall comparison of relative advantages and disadvantages of the four LID concepts are presented below.

5.3.1 No-Core LID

Advantages:

- **Simple to Construct** - With only one material used, the No-Core LID offers the simplest construction method.
- **Cost** - One of the cheapest options.

Disadvantages:

- **Durability** - Structural component of LID is washed away with each storm event. Would fail if not rebuilt between repeated storm events as was the case with Hurricane Gustav and Hurricane Ike.
- **Large Footprint** - The land-side slope is required to be 1v:5h due to the high porosity of the sand.

While the No-Core LID offers advantages in cost and construction, the questions concerning its ability to protect the GHMA raise doubts as to the viability of this LID concept.

5.3.2 Armorstone-Core LID

Advantages:

- **Simple to Construct** - Revetments are a common coastal structure, contractors with relevant experience and proper equipment will be readily available.

Disadvantages:

- **Performance** - The Armorstone-Core LID did not perform significantly differently from the No-Core LID. The armosrtone layer seemed to subside slightly during testing.
- **Large Footprint** - Even with the added protection of the armorstone layer, the sand core is required to have a land-side slope of 1v:5h.
- **Cost** - While significantly cheaper than the T-Wall, the Armorstone-Core LID is more expensive than the other options.

The Armorstone-Core LID has the same disadvantages of the No-Core LID, with added cost and construction complexity.

5.3.3 Clay-Core LID

Advantages:

- **Simple to Construct** - Clay levees are a common coastal structure, contractors with relevant experience and proper equipment will be readily available.
- **Cost** - The most affordable LID concept.
- **Performance** - The clay levee remained intact throughout the entire test.

Disadvantages:

- **Longevity** - Higher potential for core material to weaken over time.

The Clay-Core LID's combination of strong performance and low cost make it a very interesting option. The possibility of structural damage over time is possible, however clay levees are commonly used as flood control structures throughout the United States and proper maintenance procedures to ensure a long lifespan is well known.

5.3.4 T-Wall LID

Advantages:

- **Performance** - The T-Wall LID offers the best protection of all barriers. The robust design ensures that it will not fail and has proven effective in New Orleans.
- **Durability** - If sequential storms hit the GHMA, as was the case in 2008, the T-Wall LID will be able to provide protection.

Disadvantages:

- **Difficult to Construct** - More complex construction than other concepts.
- **Cost** - Substantially more expensive than any other design.

The T-Wall is by far the most robust design alternative. Already in place in New Orleans, the strong, impermeable structures are well equipped to handle hurricane conditions. However this comes at a price. The T-Wall LID costs as much as ten times the amount of other LID options considered. Further refinement of the design could cause a significant drop in cost, as the dune would inherently add substantial strength and stability, which could allow for a smaller, easier to construct T-Wall design.

REFERENCES

[1] The World Bank. GDP Growth (Annual %), April 2014. Available at http://data.worldbank.org/indicator/NY.GDP.MKTP.KD.ZG.

[2] Robbie Berg. Tropical Cyclone Report - Hurricane Ike. Technical report, National Hurricane Center, Miami, FL, 2009.

[3] William Betchart. Delta Levees - Types, Uses and Policy Options. Technical report, Delta Vision, Cupertino, CA, 2008.

[4] U.S. Census Bureau. Table 1. Annual Estimates of the Population of Metropolitan and Micropolitan Statistical Areas: April 1, 2000 to July 1, 2009, March 2010. Available at http://www.census.gov/.

[5] U.S. Census Bureau. Table 7. Cumulative Estimates of Population Change for Metropolitan Statistical Areas and Rankings: April 1, 2000 to July 1, 2009 - US Census Bureau, March 2010. Available at http://www.census.gov/.

[6] U.S. Census Bureau. Annual Estimates of the Resident Population: April 1, 2010 to July 1, 2013, March 2014. Available at http://www.census.gov/.

[7] National Geophysical Data Center. Galveston, TX, 1/3 Arc-second MHW DEM. Technical report, National Geophysical Data Center, Boulder, CO, 2007.

[8] Braja Das. Principles of Geotechnical Engineering, 8th Edition. Cengage Learning, Stamford, CT, 2014.

[9] Peter de Vries. The Bolivar Roads Surge Barrier. Master's Thesis, Delft University of Technology, Delft, Netherlands, 2014.

[10] Robert Dean and Robert Dalrymple. Coastal Processes with Engineering Applications. Cambridge University Press, Cambridge, UK, 2002.

[11] P.A. Domenico and F.W. Schwartz. Physical and Chemical Hydrogeology. John Wiley & Sons, New York, NY, 1990.

[12] Y. Goda. Random Seas and Design of Maritime Structures, 3rd Edition. World Scientific Publishing Co. Pte. Ltd., Hackensack, NJ, 2010.

[13] Hoozemans, F. and Marchand, M., and Pennekamp, H. A Global Vulnerability Analysis: Vulnerability Assessment for Population, Coastal Wetlands and Rice Production on a Global Scale. Technical report, Delft University of Technology, Delft, Netherlands, 1993.

[14] J Jin, C Jeong, KA Chang, YK Song, J Irish, and B Edge. Site Specific Wave Parameters for Texas Coastal Bridges: Final Report. Technical report, College Station, TX, 2010.

[15] Chris Jones, Larry Tanner, and Wallace Wilson. Hurricane Ike in Texas and Louisiana - Mitigation Assessment Team Report. Technical report, FEMA, Washington, DC, 2009.

[16] B. Keim and R. Muller. Spatiotemporal Patterns and Return Periods of Tropical Storm and Hurricane Strikes from Texas to Maine. Journal of Climate, 20, 2010.

[17] Diplomat Magazine. Dutch Delta Works Tour, 2014. Available at http://www.diplomatmagazine.nl/wp-content/uploads/dutch-delta-works.tour_.jpg.

[18] E P D Mansard and E R Funke. The Measurement of Incident and Reflected Spectra Using a Least Squares Method. Proceedings of 17th Intl. Conf. on Coastal Eng., 1:154–172, 1980.

[19] Ronald McPherson. Galveston Seawall Beach Nourishment Monitoring Program. Technical report, Galveston, TX, 2012.

[20] William Merrell. Ike Dike: A Coastal Barrier Protecting the Houston/Galveston Region from Hurricane Storm Surge, 2012. Available at http://www.tamug.edu/ikedike/Presentations.html.

[21] F. Moretzsohn, J. Sanchez Chavez, and J. Tunnell. Galveston Bay, 2002. Available at http://data.gulfbase.org/bay/view.php?bi.

[22] U.S. Bureau of Economic Analysis. GDP by Metro Area: Compound Annual Growth Rate, September 2013. Available at http://www.bea.gov/.

[23] U.S. Bureau of Economic Analysis. GDP by Metropolitan Area, September 2013. Available at http://www.bea.gov/.

[24] U.S. Bureau of Economic Analysis. Value Added by Industry, January 2014. Available at http://www.bea.gov/.

[25] U.S. Army Corps of Engineers Team New Orleans. St. Bernard Parish, 2013. Available at www.mvn.usace.army.mil.

[26] University of Maine. Maine Property Owner's Guide to Managing Flooding, Erosion & Other Coastal Hazards, 2014. Available at http://www.seagrant.umaine.edu/coastal-hazards-guide/beaches-and-dunes.

[27] Greater Houston Partnership. Chemicals, 2013. Available at http://www.houston.org/newgen/16_Industry_NEC/16H

[28] Greater Houston Partnership. Energy Industry Overview, 2014. Available at http://www.houston.org/newgen/16_Industry_NEC/16B

[29] Johnathan Phillips. A Sediment Budget for Galveston Bay. Department of Geography, University of Kentucky, 2004.

[30] PricewaterhouseCoopers. Economic Impacts of the Oil and Natural Gas Industry on the US Economy in 2011. Technical Report July, American Petroluem Institute, Washington, DC, 2013.

[31] Ataur Rahman and Aysha Akter. The Effect of Porosity of Submerged and Emerged Breakwater on Wave Transmission. International Journal of Environmental Science and Development, 5(5), 2014.

[32] RBR-Global, Ottawa, Ontario, Canada. WB-55 Wave Gauge User Guide, 2011. Available at rbr-global.com.

[33] RBR-Global, Ottawa, Ontario, Canada. WG-55 Wave Gauge User Manual, 1.0 edition, 2011. Available at rbr-global.com.

[34] R. Reid. USGS Research Before and After Hurricane Sandy Helps Study Coastal Changes. Civil Engineering, 2013.

[35] D. Roth. Texas Hurricane History. Technical report, National Weather Service, Camp Springs, MD, 2010.

[36] Schmitt Industries, Inc., Portland, Oregon. Acuity AccuProfile 820 Specifications, 2013.

[37] Schmitt Industries, Inc., Portland, Oregon. Acuity AccuProfile 820 User Manual, 2013.

[38] Kasper Stoeten. Applying Best Practices from the Delta Works and New Orleans to Galveston Bay. Technical report, Galveston, TX.

[39] Kasper Stoeten. Hurricane Surge Risk Reduction for Galveston Bay. Master's thesis, Delft University of Technology, Delft, Netherlands, 2013.

[40] United States Geological Survey. Storm Induced Coastal Change, 2014. Available at http://coastal.er.usgs.gov/hurricanes/coastal-change/dune-erosion.php.

[41] L. A. Taylor, B. W. Eakins, K. S. Cargignan, R. R. Warnken, T. Sazonova, and D. C. Schoolcraft. Digital Elevation Model of Galveston, Texas: Procedures, Data Sources and Analysis. Technical report, National Geophysical Data Center: Marine Geology and Geophysics Division, Boulder, CO, 2008.

[42] Robert Cory Tyler. Coastal Engineering Research Dune Start up Overview. Technical report, Texas A&M University at Galveston, Galveston, TX, 2013.

[43] U.S. Army Corps of Engineers. Engineering Manual 1110-2-1913, Design and Construction of Levees. Technical Report March 1978, US Army Corps of Engineers, Washington DC, 2000.

[44] U.S. Army Corps of Engineers. Engineering Manual 1110-2-1100, Coastal Engineering Manual. Technical report, U.S. Army Corps of Engineers, Washington DC, 2002.

[45] U.S. Department of Transportation. Highways in the Coastal Environment. Technical report, U.S. Department of Transportation, Washington DC, 2011.

[46] Anwar Zahid. T-Wall Design Example. Technical report, ARCADIS, New Orleans, 2006.

[47] Anwar Zahid. T-Wall Structural Manual. Technical report, ARCADIS, New Orleans, 2006.

APPENDIX A

SEDIMENT PARAMETERS

A.1 Sand

A.1.1 At Rest Lateral Earth Pressure

Much like a column of water exerts hydrostatic pressure on a wall, so does a column of soil which is called the at rest lateral earth pressure. The main difference is that soils have a natural angle of repose, which limits the angle at which forces are exerted. There will only be a pressure exerted on the wall if the wall is steeper than the angle of repose. With a vertical wall and sand we can evaluate the at rest lateral earth pressure for the T-Wall concept.

$$P_0 = \frac{1}{2} H^2 K_0 \gamma$$

Where P_0 is the resultant force per unit length for the at rest later earth pressure, H is the height of the sand behind the wall, K_0 is the at rest lateral earth pressure coefficient for sand, and γ is the specific weight of sand. K_0 is a factor of the angle of repose and can be calculated by:

$$K_0 = (1 - \sin(\phi)) ocr^{\sin(\phi)}$$

Where ϕ is the angle of repose, and ocr is the overconsolidation ratio, which in the case of sand is 1. Plugging in known quantities for sand and our design height, we get:

$$K_0 = (1 - \sin(30))1^{\sin(30)} = 0.5$$

$$P_0 = \frac{1}{2}(17\,\text{ft})^2(0.5)(130.5\,\frac{\text{lbs}}{\text{ft}^3}) = 9,430\,\frac{\text{lbs}}{\text{ft}}$$

A.2 Determining Soil Parameters for Clay

A.2.1 Liquid Limit

To determine the liquid limit of the Campeche Clay used in physical modeling, the "Casa Grande" blows test was used. [8] Results are plotted in Figure A.1.

Moisture content is calculated with the following equation with the variables explained in Table A.1.:

$$w(\%) = \frac{M_2 - M_3}{M_3 - M_1}(100)$$

Table A.1: Data obtained for Liquid Limit calculation.

Test	1	2	3
Mass of Can, M_1 [g]	32.7	32.5	32.7
Mass of Can + Moist Soil, M_2 [g]	44.5	45.9	51.8
Mass of Can + Dry Soil, M_3 [g]	40.1	40.8	44.7
Moisture Content [%]	59.5	61.4	59.2
Number of Blows	33	35	25

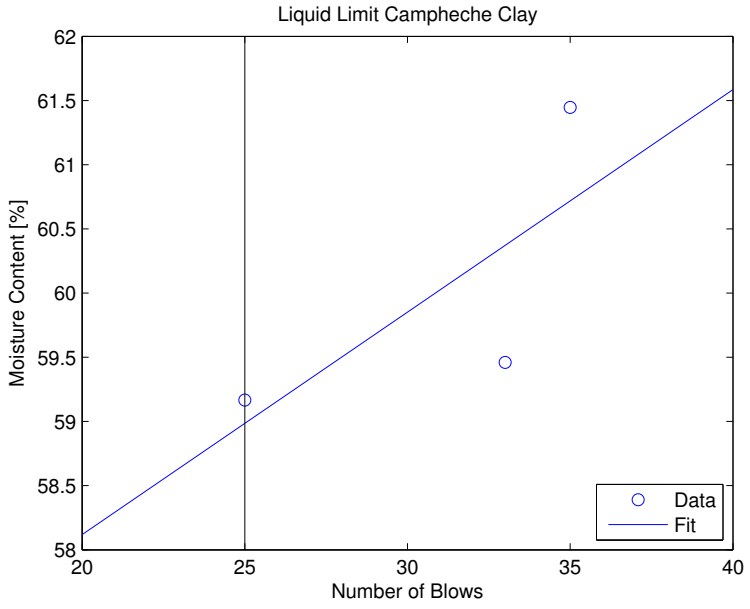

Figure A.1: Plot of moisture content vs. number of blows for liquid limit test results reported in Table A.1.

The liquid limit is then determined to be 59% using a first-degree polynomial fit and solving for the moisture content of 25 blows. Fit parameters are $m = 0.1733$, $b = 54.65$ where $y = mx + b$.

A.2.2 Plastic Limit

To determine the plastic limit of the Campeche Clay used in physical modeling, the "Hand Roll" test was used, with results shown in Table A.2. [8]

Moisture content is calculated with the following equation:

$$w(\%) = \frac{M_2 - M_3}{M_3 - M_1}(100)$$

Table A.2: Data obtained for Plastic Limit calculation.

Mass of Can, M_1 [g]	32.6
Mass of Can + Moist Soil, M_2 [g]	50.0
Mass of Can + Dry Soil, M_3 [g]	46.5
Moisture Content [%]	25

Therefore the plastic limit was calculated to be 25%.

The Plasticity Index, PI is then:

$PI = LL - PL = 59\% - 25\% = 34\%$

A.2.3 Shear Strength

To determine the shear strength of the Campeche Clay used in physical modeling, the Unconfined Compression test was used. [8]

Note that the specimen used was completely dry (moisture content assumed 0%) and beginning to crack.

For this test, the specimen had a diameter $D = 2.5\,\text{in}$, length $L = 4.25\,\text{in}$ and the calibration factor was $0.702\,{}^{\text{lbs}}/_{\text{div}}$.

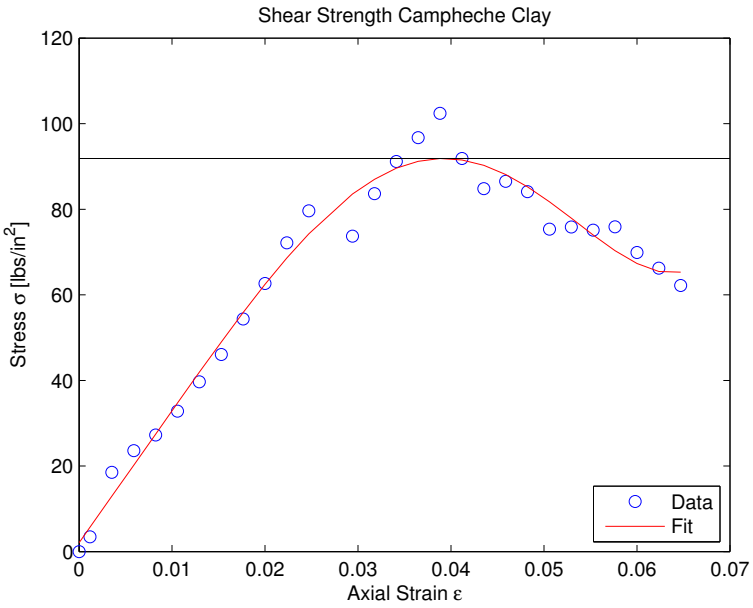

Figure A.2: Plot of σ vs. ϵ for the Unconfined Compression test results.

Results are plotted in Figure A.2 along with a polynomial fit. Taking the peak of the fit curve, the unconfined compression strength of the Campeche Clay at 0% moisture is calculated to be $\underline{92\,{}^{lbs}/_{\text{in}^2}}$. To find the shear strength of the soil, the unconfined compression strength is simply divided by a factor of two. [8]

APPENDIX B

INSTRUMENT SPECIFICATIONS

More detailed information on the wave gauges and laser profiler used in this study are provided in the section below.

B.1 RBR WG-55 Wave Gauges

Specifications for the WG-55 provided by RBR [32]:

- Linearity: 0.15% of full scale
- Accuracy: 0.15% of full scale
- Air Temperature Coefficient: 0.03% of full scale per °C
- Water Temperature Coefficient: 0.03% of full scale per °C
- Operating Temperature: -10 °C to 50 °C
- Time Response: 5 ms
- Output Signal: -5 Vdc to 5 Vdc
- Power Supply: 8 Vdc to 20 Vdc
- Power Consumption: 21 mA at 10 V

B.2 Acuity AP820-1000 Laser Scanner

Figures B.1 and B.2 provide detailed specifications and a schematic of the Acuity AP820-1000 used for physical modeling experiments of this study.

AP820 Model Specifications in mm [in.]

Model	-5	- 20	- 40	- 60	- 80	- 120	- 240	- 400	-1000
Range in Z-axis	5.9 [0.23]	20 [0.79]	40 [1.6]	60 [2.4]	80 [3.2]	120 [4.7]	240 [9.5]	400 [15.7]	1000 [39.4]
Range Beginning	38 [1.5]	53 [2.1]	50 [2.0]	53 [2.1]	60 [2.4]	84 [3.3]	220 8.7]	330 [13.0]	550 [21.7]
Range End	43.9 [1.7]	73 [2.9]	90 [3.5]	113 [4.5]	140 [5.5]	204 [8.0]	460 [15.7]	730 [28.7]	1550 [61.0]
Linearity, Z & X axis	+/- 0.06% of the Z range								
µm [10⁻³ in.]	3.5 [0.14]	12 [0.47]	24 [0.95]	36 [1.4]	48 [1.9]	72 [2.8]	144 [5.7]	240 [9.4]	630 [25]
Resolution Z & X axis, µm [10⁻³ in.]	3.0 [0.12]	11 [0.43]	19 [0.75]	31 [1.2]	42 [1.7]	63 [2.5]	112 [4.4]	213 [8.4]	600 [24]
Field of View X-axis @ Range Beginning	3.9[0.15]	10 [0.39]	20 [0.79]	30 [1.2]	40 [1.6]	60 [2.4]	120 [4.7]	200 [7.9]	500 [19.7]
@ Range End	5.0 [0.20]	13 [0.51]	27 [1.1]	40 [1.5]	55 [2.2]	80 [3.2]	160 [6.3]	280 [11.0]	800 31.5]
Scan frequency	up to 200 Hz (profiles / s) for the full Range								
Weight (less cables) g [oz.]	295 [10.3]	273 [9.6]	290 [10.2]	290 [10.2]	290 [10.2]	430 [15.2]	710 [25.0]	1100 [38.8]	2000 [70.5]
Laser	658 nm, visible RED, Class 2M					658 nm, visible RED, Class 3R			NA
	405 nm,visible BLUE, Class 3R						NA	NA	NA
	NA						435 nm, Blue, 3R		Blue, 3B
Power	10 - 30 VDC, 4-8 W max consumption (Suggest 12 - 24 V)								
Environmental	0° to 40°C [32° to 104°F], With cooling option to 400°C [752°F]; Humidity: < 90% RH								
Vibration	5.5 g @ 1 kHz								
Enclosure Protection	IP64, Keep optical windows clean for best performance. Aluminum case.								
Data Interface	Ethernet Reports: 2D Profile Data, Encoder postion, Status, Temperature, Clock counter, Version #, Switch-on counter								
Signal Inputs	Digital, Incremental Encoder Position Synchronization IN/OUT for Multiple Sensors								
Connector 1	Ethernet: M12 round, 4 pin, D-coded, female								
Connector 2	Power & Synchronization: M12 round, 8 pin, A-coded, male								
Cables	Ethernet: 2m cable, CAT 5, RJ45 termination Power / Serial: 2m cable, Polyurethane jacket, 9 conductor								

White [pin 1]	+10 - 30 V DC	Yellow [pin 4]	Digital input 2 / Position	Blue [pin 7]	TxD
Brown [pin 2]	Digital input 1 / Position	Gray [pin 5]	Sync OUT	Red [pin 8]	RxD
Green [pin 3]	GND, 0V	Orange [pin 6]	Sync IN / Hardware trigger	Screen	Tied to connector plug housing

* Each sensor model has unique dimensions.

Figure B.1: AP820-1000 laser scanner specifications. [36]

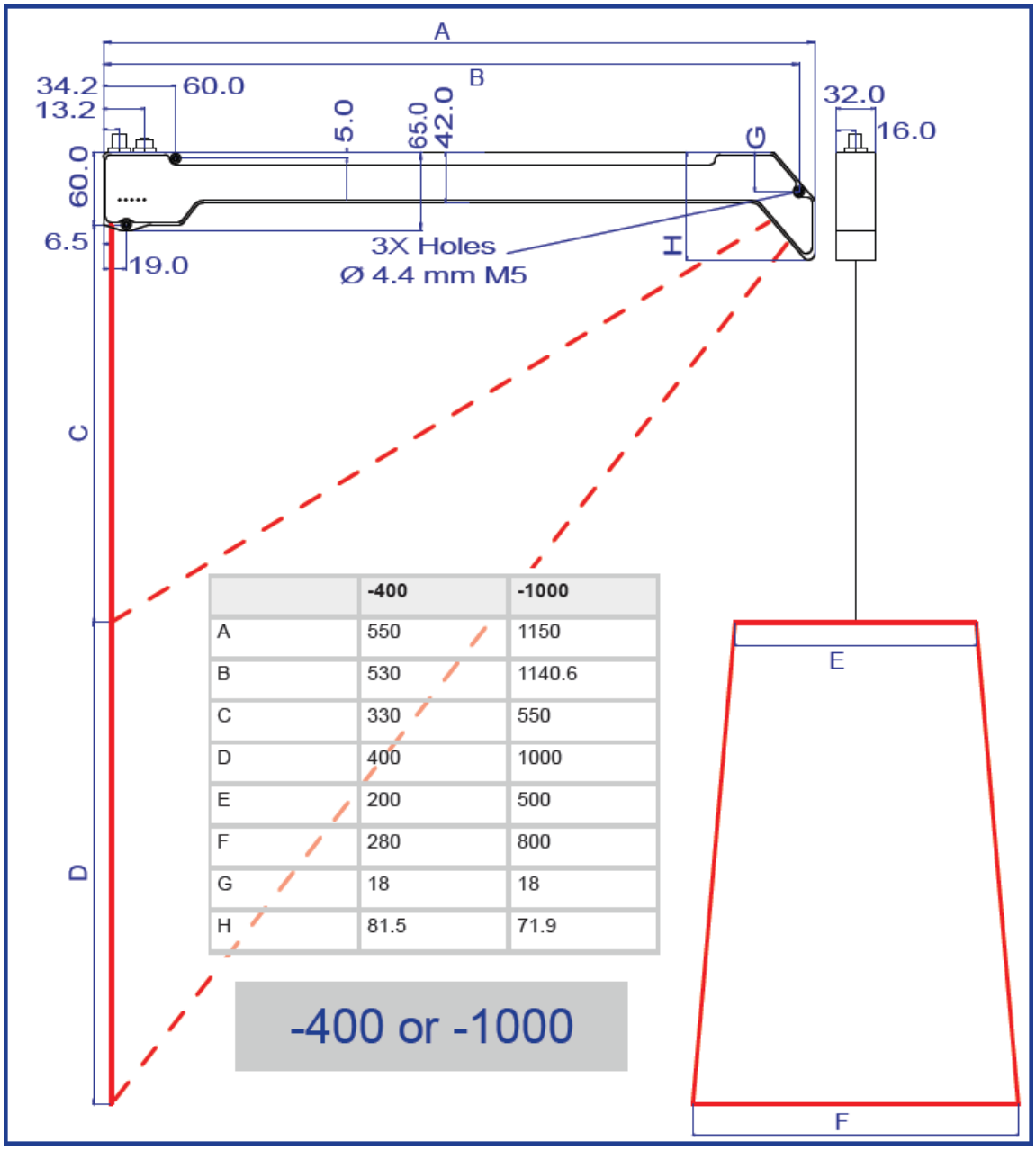

	-400	-1000
A	550	1150
B	530	1140.6
C	330	550
D	400	1000
E	200	500
F	280	800
G	18	18
H	81.5	71.9

Figure B.2: AP820-1000 laser scanner dimensions and schematic. The table lists dimensions for both the AP820-400 and AP820-1000 models. [36]

APPENDIX C

ADDITIONAL PROFILE SCANS

Figures C.1 - C.3 show beach profiles for all LID configurations after 5 min, 10 min, and 20 min, respectively. These figures show intermediate beach profiles between Figures 4.11 and 4.12 in Section 4.3.1.

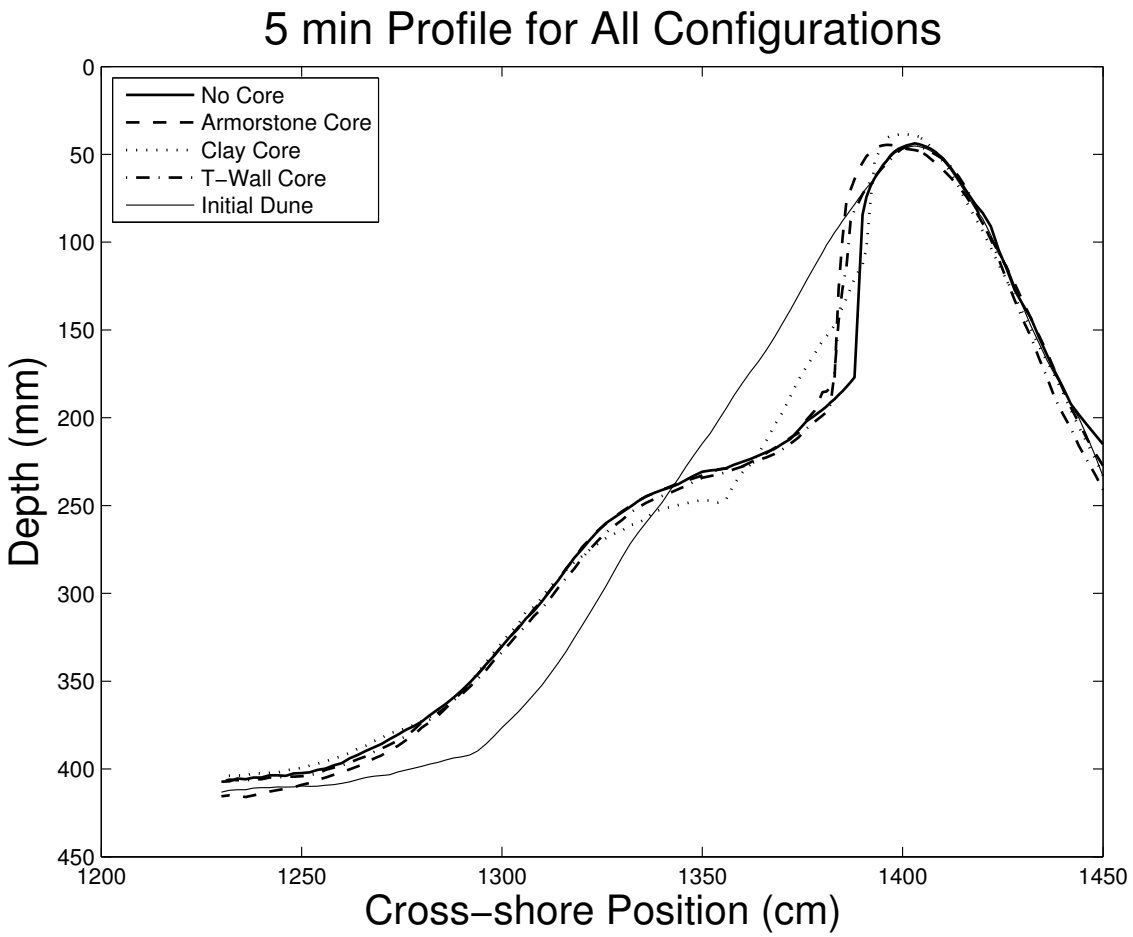

Figure C.1: Profile scans after 5 min for each LID.

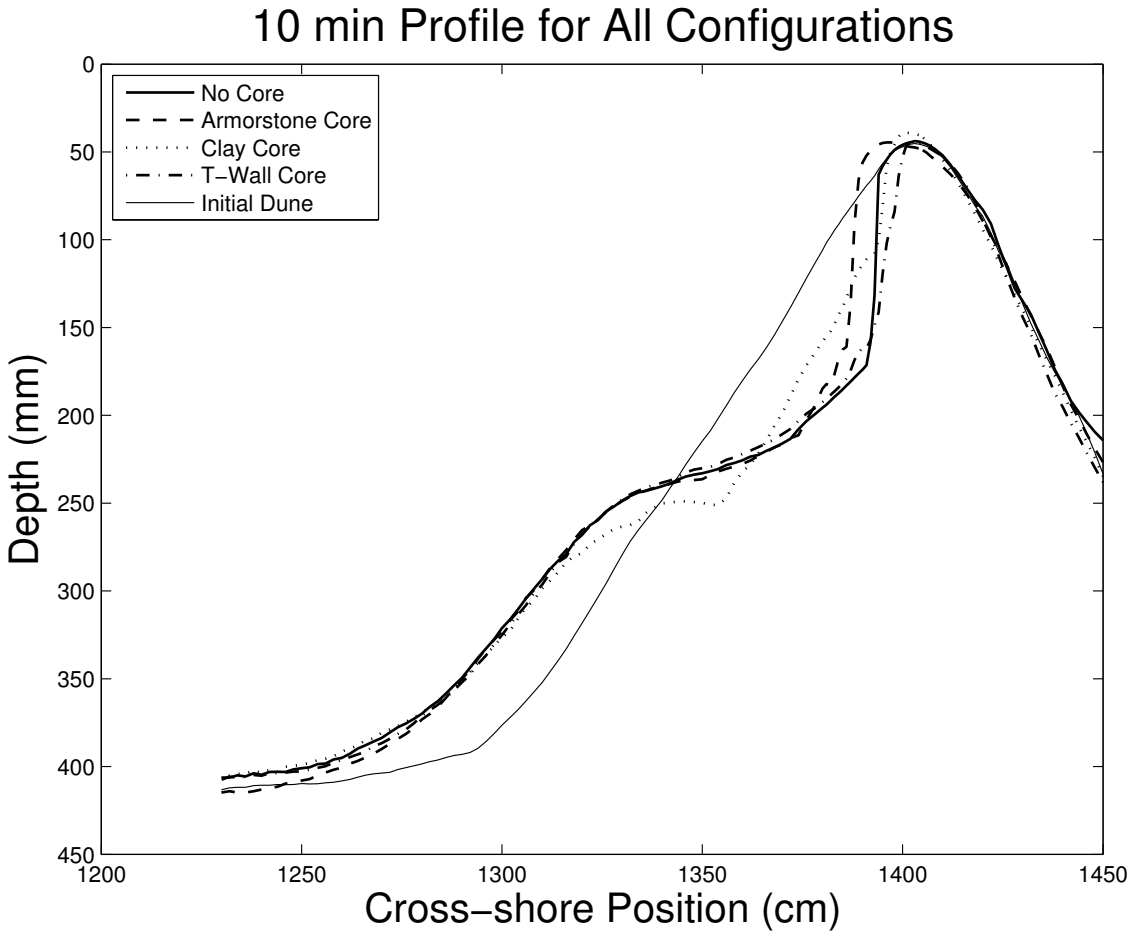

Figure C.2: Profile scans after 10 min for each LID.

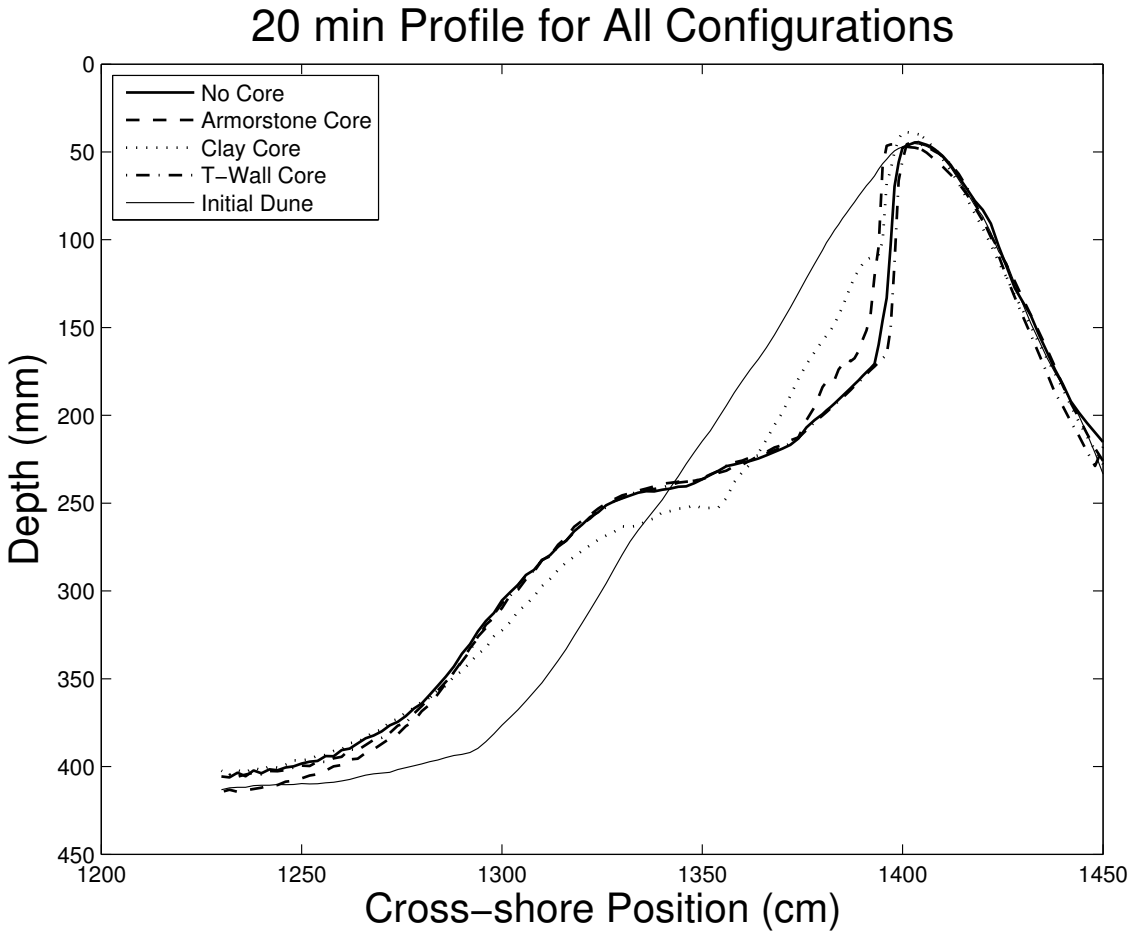

Figure C.3: Profile scans after 20 min for each LID.